



HHS Public Access

Author manuscript

J Proteomics. Author manuscript; available in PMC 2017 January 01.

Published in final edited form as:

J Proteomics. 2015 January 01; 112: 190–209. doi:10.1016/j.jprot.2014.08.016.

Proteomics of apheresis platelet supernatants during routine storage: Gender-related differences

Monika Dzieciatkowska^{a,1}, Angelo D'Alessandro^{a,1}, Timothy A. Burke^{b,1}, Marguerite R. Kelher^b, Ernest E. Moore^c, Anirban Banerjee^d, Christopher C. Silliman^{b,c,d}, Bernadette F. West^b, and Kirk C. Hansen^{a,*}

^aBiochemistry and Molecular Genetics, School of Medicine, University of Colorado Denver, Anschutz Medical Campus, Aurora, CO, United States

^bBonfils Blood Center, Denver, CO, United States

^cSurgery, School of Medicine, University of Colorado Denver, Anschutz Medical Campus, Aurora, CO, United States

^dPediatrics, School of Medicine, University of Colorado Denver, Anschutz Medical Campus, Aurora, CO, United States

Abstract

Proteomics has identified potential pathways involved in platelet storage lesions, which correlate with untoward effects in the recipient, including febrile non-haemolytic reactions. We hypothesize that an additional pathway involves protein mediators that accumulate in the platelet supernatants during routine storage in a donor gender-specific fashion.

Apheresis platelet concentrates were collected from 5 healthy males and 5 females and routinely stored. The 14 most abundant plasma proteins were removed and the supernatant proteins from days 1 and 5 were analyzed via 1D-SDS-PAGE/nanoLC-MS/MS, before label-free quantitative proteomics analyses. Findings from a subset of 18 proteins were validated via LC-SRM analyses against stable isotope labeled standards.

A total of 503 distinct proteins were detected in the platelet supernatants from the 4 sample groups: female or male donor platelets, either at storage day 1 or 5. Proteomics suggested a storage and gender-dependent impairment of blood coagulation mediators, pro-inflammatory complement components and cytokines, energy and redox metabolic enzymes. The supernatants from female donors demonstrated increased deregulation of structural proteins, extracellular matrix proteins and focal adhesion proteins, possibly indicating storage-dependent platelet activation.

*Corresponding author at: Department of Biochemistry and Molecular Genetics, University of Colorado Health Sciences Center, 12801 East 17th Ave., Aurora, CO, United States. Tel.: +1 303 724 5544.

¹Co-first authors.

Supplementary data to this article can be found online at <http://dx.doi.org/10.1016/j.jprot.2014.08.016>.

Conflict of interest: The authors disclose no conflict of interest.

Transparency Document: Transparency Document associated with this article can be found, in the online version.

Routine storage of platelet concentrates induces changes in the supernatant proteome, which may have effects on the transfused patient, some of which are related to donor gender.

Biological significance—The rationale behind this study is that protein components in platelet releasates have been increasingly observed to play a key role in adverse events and impaired homeostasis in transfused recipients.

In this view, proteomics has recently emerged as a functional tool to address the issue of protein composition of platelet releasates from buffy coat-derived platelet concentrates in the blood bank. Despite early encouraging studies on buffy coat-derived platelet concentrates, platelet releasates from apheresis platelets have not been hitherto addressed by means of extensive proteomics technologies. Indeed, apheresis platelets are resuspended in donors' plasma, which hampers detection of less abundant proteins, owing to the overwhelming abundance of albumin (and a handful of other proteins), and the dynamic range of protein concentrations of plasma proteins.

In order to cope with these issues, we hereby performed an immuno-affinity column-based depletion of the 14 most abundant plasma proteins. Samples were thus assayed via GeLC-MS, a workflow that allowed us to cover an unprecedented portion of the platelet supernatant proteome, in comparison to previous transfusion medicine-oriented studies in the literature.

Finally, we hereby address the issue of biological variability, by considering the donor gender as a key factor influencing the composition of apheresis platelet supernatants. As a result, we could conclude that platelet supernatants from male and female donors are not only different in the first place, but they also store differently. This conclusion has been so far only suggested by classic transfusion medicine studies, but has been hitherto unsupported by actual biochemistry/proteomics investigations.

In our opinion, the main strengths of this study are related to the analytical workflow (immunodepletion and GeLC-MS) and proteome coverage, the translational validity of the results (from a transfusion medicine standpoint) and the biological conclusion about the intrinsic (and storage-dependent) gender-related differences of platelet supernatants.

Keywords

Donor; Transfusion medicine; Proteomics; Human; Label-free quantitation; Mass spectrometry

1. Introduction

Platelets (PLTs) are key mediators of hemostasis, and PLT concentrates (PCs) are an important component of supportive care for thrombocytopenic patients. Despite decades of improvements, preparation of PLT concentrates still represents one of the major challenges to the blood bank, in light of standard platelets storage limitations [1–3]. Indeed, routine storage results in decreased PLT morphology scores (loss of disk shape) and responses to agonist (shape change), increased hypotonic shock response, volume and density heterogeneity, PLT activation marker expression (e.g. CD62P, PAC-1 binding/ expression of the fibrinogen binding site on the α IIb β 3 complex), release of PLT α -granules, cytosolic proteins and inflammatory mediators, increased pro-coagulant activity, and altered supernatant pH and glycoprotein expression [1–4].

In most countries, PCs are stored for 5–7 days, depending on the national guidelines. This short lifespan results in a significant amount of the PLT inventory becoming outdated and discarded. Lifespan limitations also impose constraints regarding the narrow time window to complete donor testing, shipment of PCs, and leaves even less time for the recipient hospitals to transfuse these units.

Proteomics is an ideal tool to investigate *in vitro* changes of stored PLTs [5]. Owing to their anucleate nature, platelets have limited protein synthesis capacity [6] and a rather stable proteome (~5,000 proteins) that, in comparison to other cell types, is less affected by biological variability issues [7–10]. Translational application of proteomics to PLT-related transfusion medicine issues has focused on many aspects of PLT product preparation, including the effects of preparation (cell processing and pathogen inactivation) on *in vivo* viability [11–18].

PLT supernatants are recognized mediators of hypercoagulability after injury [19], as they become increasingly enriched with PLT releasates [20], lipid [21] and oncogenic, angiogenic and invasion-promoting mediators [22,23]. In this view, it has become increasingly accepted that protein components in PLT releasates might play a non-secondary biological role in mediating untoward responses in the recipients [24]. Despite recent breakthroughs, the intrinsic limitations of the gel-based approaches [5,25] (limited coverage of the proteome, impaired detection of very high molecular weight and hydrophobic proteins) leave room for further improvements in this research endeavor, with evident benefit for the transfusion community.

In the present study we hypothesize that a significant number of proteins accumulate during routine PLT storage which are directly affected by donor gender and may in turn affect the recipient. The differences in male and female donors were addressed at the two extreme storage time points, as to assess whether the PLT proteomes of freshly donated apheresis PLTs differed as a function of storage time, either in a storage or gender-dependent fashion.

2. Materials and methods

2.1. Sample collection

After obtaining informed consent under a protocol approved by the Combined Multiple Institution Review Board, 10 healthy donors (5 females –mean age: 54.0 ± 5.7 and 5 males – mean age 47.7 ± 1.2) donated one unit of apheresis platelets using a Cobe Trima apparatus with appropriate leukoreduction ($<5 \times 10^6$ /unit per Bonfils Blood Center standard operating procedures and consistent with AABB guidelines, as determined by direct leukocyte counting by flow cytometry). Duration of the apheresis procedure was 92.0 ± 2 and 97.3 ± 1.5 min for female and male donors, respectively. All of the donors gave double, with one donating a triple, apheresis units. So the platelet numbers are all a total of 6×10^{11} with one being 9×10^{11} by definition and cutoffs. All the females were post-menopausal; none on hormone replacement. Samples were taken serially on days 1 and 5 via sterile couplers and centrifuged first at 5,000 g for 7 min to remove the majority of platelets and centrifuged again at 12,500 g for 6 min to remove all platelets and acellular debris. The supernatants

were aliquoted and stored at -80°C . All samples were prepared by the identical protocol. Therefore, artifacts caused by preparation should affect all samples similarly.

2.2. QConCAT design and expression

In agreement with Pratt et al. [26], QConCAT constructs were designed to quantify plasma and PLTs specific proteins. The selection of target peptides was based on the result of previous non-targeted experiments of plasma and publicly accessible databases, including PeptideAtlas (www.peptideatlas.org) SRM Atlas (www.srmatlas.org) and Global Proteome Database (<http://gpmdb.thegpm.org/>). The QConCAT DNA construct was synthesized de novo and cloned into pET21a by Genscript (Piscataway, NJ). E. coli strain BL21(l)DE3 was transformed with the vector and cultured in minimal medium supplemented either with unlabeled or $^{13}\text{C}_6$ arginine and $^{13}\text{C}_6$ lysine at 0.1 mg/ml (Sigma Aldrich). The cells were grown to mid log phase (A_{600} 0.6–0.8), at which point expression was induced by adding 1 mM isopropyl-D-1-thiogalactopyranoside. The cells were lysed with the BugBuster Protein Extraction Reagent (EMD Millipore). Inclusion bodies were suspended in 20 mM phosphate buffer, 6 M guanidinium chloride, 0.5 M NaCl, 20 mM imidazole, pH 7.4. QConCAT proteins were purified by affinity chromatography using a nickel-based resin. The purified QConCAT was desalted by three rounds of dialysis against 100 volumes of 10 mM ammonium bicarbonate, pH 8.5.

2.3. Depletion of the most 14 abundant plasma proteins in platelet supernatants and protein digestion

Multiple Affinity Removal SystemTM columns (4.6×100 mm) designed to deplete 14 abundant plasma proteins (albumin, IgG, antitrypsin, IgA, transferrin, haptoglobin, fibrinogen, alpha2-macroglobulin, alpha1-acid glycoprotein, IgM, apolipoprotein AI, apolipoprotein AII, complement C3, and transthyretin) were purchased from Agilent (Palo Alto, CA). Depletion was performed at room temperature on an AKTAMicro (GE Healthcare Life Sciences) system. Platelet supernatant samples were diluted fourfold using the load/wash buffer supplied by the manufacture and remaining particulates in the diluted supernatants were removed by centrifugation through a 0.22- μm spin filter 1 min at $16,000 \times g$. After equilibration with the load/wash buffer, the Multiple Affinity Removal SystemTM column was loaded with 160 μL of the diluted plasma at a low flow rate ($0.125 \text{ mL min}^{-1}$) for 4 min. Flow-through fractions, representing depleted platelet supernatants were collected and saved. The bound proteins were released with elution buffer at 1.0 mL/min for 10 min. The column was then washed with the load/wash buffer for 11 min at a flow rate of 1 mL/min . Each depletion cycle took 38 min of total run time. Each flow-through portion was individually concentrated using 5000 Da molecular weight cutoff spin concentrators (Agilent Technologies, Palo Alto, CA), followed by buffer exchange with 50 mM NH_4HCO_3 and protein concentrations were determined by a Bradford protein assay.

In agreement with Dziewiatkowska et al. [27], a portion of the sample (30 μg) was diluted into SDS-PAGE sample buffer, heated at 70°C for 10 min and loaded in a single lane on a 1.5-mm-thick 4–12% Bis-Tris gel (Invitrogen). After separation, the gel was stained with SimplyBlue SafeStain (Invitrogen). Each lane of the gel was divided into 24 equal-sized bands and proteins in the gel were digested as follows. Bands were destained in 200 μL of 25

mM ammonium bicarbonate in 50 % v/v ACN for 15 min, and then 200 μ l of 100% ACN was applied for 15 min at room temperature. Dithiothreitol (DTT) was added to a final concentration of 10 mM and incubated at 65 °C for 30 min to reduce the disulfide bonds. Protein cysteines were alkylated with 55 mM iodoacetamide for 30 min at room temperature in the dark. The iodoacetamide was then removed, and washes were performed with 200 μ l of distilled water followed by addition of 100 μ l of ACN. Then ACN was removed, and 50 μ l of the 0.01 μ g/ μ l trypsin solution was added to each plug. The gel plugs were allowed to rehydrate at 4 °C for 30 min and then placed at 37 °C and allowed to digest overnight. The tryptic mixtures were acidified with formic acid up to a final concentration of 1%. Peptides were extracted three times from the gel plugs using 50% ACN, 1% FA, concentrated under vacuum (SpeedVac, Savant ThermoFisher) to approximately \sim 20 μ L, and subjected to LC-MS/MS analysis. If necessary, they were stored at -20 °C.

2.3.1. Targeted quantitation assay via single reaction monitoring—For all targeted quantification analyses, a subset of three (out of five of the label-free approach) male and female units of platelet supernatants after days 1 and 5 of storage were analyzed independently with the isotopic QConCAT standard. For trypsin proteolysis, known amounts of the recombinant isotopically labeled QConCAT protein were mixed with the albumin and IgG depleted platelets supernatant. The samples were reduced, alkylated, and digested with sequencing grade modified trypsin (Promega) according to the FASP protocol using a 10 kDa molecular weight cutoff filter. In brief, samples were mixed in the filter unit within 8 M urea in 0.1 M Tris-HCl, pH 8.5 and centrifuged at 14000 *g* for 15 min. The proteins were reduced by addition of 100 μ L of 10 mM DTT in 8 M urea in 0.1 M Tris-HCl, pH 8.5, incubation for 30 min at RT and the device was centrifuged. Subsequently, 100 μ l of 55 mM iodoacetamide in 8 M urea in 0.1 M Tris-HCl, pH 8.5 were added to the samples, incubation for 30 min at RT in dark followed by centrifugation. Afterward, three washing steps with 100 μ L of 8 M urea in 0.1 M Tris-HCl, pH 8.5 solution were performed, followed by three washing steps with 100 μ L of 50 mM ABC buffer. Proteins were digested with trypsin overnight at 37 °C. Peptides were recovered from the filter using 30% ACN. The volume of the eluted sample was reduced to \sim 2 μ L in a vacuum centrifuge and reconstituted to 50 μ L with 0.1% formic acid. Following digestion, the resultant peptide mixture was analyzed in duplicate by LC-SRM. Further details about the peptides are provided in the Supplementary File 1.

2.4. Liquid chromatography-tandem mass spectrometry

Samples were analyzed on an LTQ Orbitrap Velos mass spectrometer (Thermo Fisher Scientific) coupled to an Eksigent nanoLC-2D system through a nanoelectrospray LC - MS interface. A volume of 8 μ L of sample was injected into a 10 μ L loop using the autosampler. To desalt the sample, material was flushed out of the loop and loaded onto a trapping column (ZORBAX 300SB-C18, dimensions 5 \times 0.3 mm 5 μ m) and washed with 0.1% FA at a flow rate of 5 μ L/min for 5 min. The analytical column was then switched on-line at 600 nL/min over an in house-made 100 μ m i.d. \times 150 mm fused silica capillary packed with 4 μ m 80 Å Synergi Hydro C18 resin (Phenomex; Torrance, CA). After 10 min of sample loading, the flow rate was adjusted to 350 nL/min, and each sample was run on a 90-min linear gradient of 5–40% ACN with 0.1% formic acid to separate the peptides. LC mobile phase

solvents and sample dilutions used 0.1% formic acid in water (Buffer A) and 0.1% formic acid in acetonitrile (Buffer B) (Chromasolv LC–MS grade; Sigma-Aldrich, St. Louis, MO). Data acquisition was performed using the instrument supplied Xcalibur™ (version 2.1) software. The mass spectrometer was operated in the positive ion mode. Each survey scan of m/z 400–2,000 was followed by collision-assisted dissociation (CAD) MS/MS of twenty most intense precursor ions. Singly charged ions were excluded from CID selection. Normalized collision energies were employed using helium as the collision gas.

2.5. Selected reaction monitoring analysis

A targeted Selected Reaction Monitoring (SRM) approach was performed using the QTRAP® 5500 interfaced with a capillary HPLC system (Agilent 1200, Palo Alto, Calif). 10 μ l of each sample was injected and directly loaded onto an Agilent C18 column (Zorbax SB-C18, 5 μ m 150 \times 0.5 mm) with 5% ACN, 0.1% FA at 30 μ l/min for 3 min. Chromatography was performed with Solvent A (Milli-Q water with 0.1% formic acid) and Solvent B (acetonitrile with 0.1% formic acid). A gradient of 5–28% ACN was run for 61 min to differentially elute QConCAT peptides. The mass spectrometer was run in positive ion mode with the following settings: a source temperature of 200 °C, spray voltage of 5300 V, curtain gas of 20 psi, and a source gas of 35 psi (nitrogen gas). Multiple MRM transitions were monitored using unit resolution in both Q1 and Q3 quadrupoles to maximize specificity. SRM assay optimization was performed with the aid of Skyline v1.2 software [28]. Collision energies (CE) and declustering potential (DP) were optimized for each transition. The energy was ramped around the predicted value in 5 steps on both sides with 1 V increments. Method building and acquisition were performed using the instrument supplied Analyst® Software (Version 1.5.2). Each sample was run in duplicate.

2.6. Data analysis

MS/MS spectra were extracted from raw data files and converted into mgf files using a PAVA script (UCSF, MSF, San Francisco, CA). These mgf files were then independently searched against Human IPI database using an in-house Mascot™ server (Version 2.2.06, Matrix Science). Mass tolerances were \pm 15 ppm for MS peaks, and \pm 0.6 Da for MS/MS fragment ions. Trypsin specificity was used allowing for 1 missed cleavage. Met oxidation, protein N-terminal acetylation, and peptide N-terminal pyroglutamic acid formation were allowed for variable modifications while carbamidomethylation of Cys was set as a fixed modification. Alternative searches were performed indicating semi-trypsin digestion, while maintaining the other search criteria unaltered. Scaffold (version 4.3.2, Proteome Software, Portland, OR, USA) was used to validate MS/MS based peptide and protein identifications. All mascot DAT files, for each subject (10 bands each) were loaded together as one “biological sample” within Scaffold. Peptide identifications were accepted if they could be established at greater than 95.0% probability as specified by the Peptide Prophet algorithm. Protein identifications were accepted if they could be established at greater than 99.0% probability and contained at least two identified unique peptides in the first set of experiments.

All data files generated on the triple quadrupole mass spectrometer during LC-SRM analyses were imported to Skyline v2.2 software for data processing. Quantification was

based on the ratio of corresponding light and heavy peak areas. The peak integration was done automatically by the software, using Savitzky-Golay smoothing, and all the data were manually inspected to confirm correct peak detection.

2.6.1. Heat maps and clustering—Quantitative results from Scaffold or Skyline were exported into .xls files and loaded into GENE-E (v. 3.0.200 - Broad Institute, Inc.) to plot heat maps and perform hierarchical clustering analyses (one minus Pearson correlation). Raw results were Z-score normalized and heat maps were plotted as to regroup proteins showing (1.5 fold change) increases or decreases in a gender or storage day-dependent fashion. Gene ontology annotations for biological functions and cell compartments were performed either with Scaffold or David v. 6.7 (David Bioinformatics services).

3. Results

A total of 503 distinct proteins were detected in the platelet supernatants from the 4 sample groups: female or male at storage day 1 or 5. Proteins are enlisted in Table 1, together with the IPI identification numbers, the theoretical molecular weight and the mean quantitative emPAI values as calculated for each of the four groups. These quantitative results were thus exported for hierarchical clustering analysis (1-Pearson correlation), as graphed in Supplementary Fig. 1.

In order to ease data analysis and interpretation, we thus exported sub-clusters either including proteins:

- i. constitutively higher in the supernatants of PLTs from female (Fig. 1.A) or male (Fig. 1.B) donors, not affected by storage duration;
- ii. decreasing or increasing (Supplementary Table 2) from storage day 1 to day 5 both in PLTs from female and male donors (Fig. 2.A and B, respectively);
- iii. decreasing in a storage-dependent fashion in female (Fig. 3.A) or male (Fig. 3.B) PLT supernatants only;
- iv. increasing in a storage-dependent fashion in female (Fig. 4.A) or male (Fig. 4.B) PLT supernatants only;
- v. showing storage-dependent reverse trends in a gender-specific fashion (Fig. 5).

Bioinformatic elaboration for functional GO term enrichment via DAVID is reported for each of these groups in Supplementary Table 1 (except group (v), owing to the limited number of entries). The observed proteins were primarily grouped into secreted extracellular (GO:0005576) proteins of the platelet granules (GO:0031091) and granule lumen (GO:0031093), other than membrane-bound proteins (GO:0031988) gene ontology groups (Supplementary Table 1).

It is worth noting that parallel increases and decreases in the levels of different proteins involved in the same biological pathways were observed, both when addressing the storage

and the gender effect on the proteomes of apheresis PLT supernatants (Supplementary Table 1). Indeed, we identified either female or male, storage day 1 or day 5 specific proteins involved in endopeptidase inhibitor activity (GO:0004866) or blood coagulation (GO:0007596). This might be due also to the different half-lives of proteins originally present in plasma supernatants of apheresis PLTs, or proteins shed through PLT releasates or from trace amounts of contaminating cells (such as WBCs) over storage progression. Additionally, it should be noted that although protein extraction has been performed using a widely accepted procedure [20,29,30], PLT centrifugation steps in the absence of prostacyclin might have promoted release of PLT proteins in the supernatant, thereby affecting the supernatant proteome profiles to some extent, both in PLTs from male and female donors.

3.1. LC-SRM targeted quantitative validation against QConCAT standards

Despite the exploratory nature of the study, we validated results for a subset of 18 proteins using LC-SRM targeted assays against stable isotope labeled peptides. Proteins were selected on the basis of relative trends in label-free analyses (Fig. 6.A), including five proteins increasing in apheresis PLT supernatants during storage duration (CXCL7, PLF4, GPV, THBS1, SRGN – UniProt gene names), six proteins constitutively higher in samples from female (FGB, A2M, APOA1, CRP, F13B) or male donors (HBA1, HBB, CA1, CLU, vWF, TTR) or a protein decreasing during storage duration (Fig. 6.B). An example of the skyline workflow is provided in Supplementary Fig. 2. Despite the limited number of biological and technical replicates of the untargeted label-free approach, targeted quantitation confirmed trends for most of the selected proteins. A discrepancy was observed for Vitamin K-dependent protein S (PROS1), possibly resulting from technical caveats associated with the less accurate label-free semi-quantification approach used in the untargeted experiments. Indeed, PROS1 decreased in a storage-dependent fashion in both label free (Fig. 6.A) and targeted assays (Fig. 6.B). However, PROS1 appeared to be 14% higher in day 1 female donor supernatants in comparison to day 1 male in the label free assays, while in targeted analyses it was measured as 20% higher in the day 1 male group. Analogous observations were made for C-reactive protein (CRP) and vWF, with constitutively higher levels in female and male donor supernatants, respectively, in targeted analyses, while in label free analyses they decreased or increased in a storage-dependent fashion, respectively.

3.2. Gender-specificity of PLT supernatants

Apheresis PLT supernatants were characterized by genderspecific proteins (Fig. 1). For example, the isoform 1 of pregnancy zone protein, a carrier and modulator of placental protein-14 in T-cell growth and cytokine production that is associated with late pregnancy [31], was identified only in female donor supernatants (Fig. 1.A). Female apheresis PLT supernatants were characterized by the highest storage-dependent increase in protein concentrations. A subset of female-specific PLT alterations were classified as involved in cell adhesion (GO:0007155 - Supplementary Table 1 - insulinlike growth factor-binding protein complex acid labile subunit isoform 1, angiopoietin-related protein 3, cadherin-1, Isoform 1 of A disintegrin and metalloproteinase with thrombospondin motifs 13, hyaluronan-binding protein 2 – Fig. 1.A). On the other hand, apheresis PLT supernatants

from male donors were enriched in antimicrobial proteins (e.g. cathelicidin, cathepsin D and Z, dermicidin) and inflammation/immune responses (attractin, immunoglobulins and complement components), iron transporters (haptoglobin, transthyretin - TTR and serotransferin, despite the latter two proteins being previously depleted by affinity chromatography), apolipoproteins/serum amyloid proteins (apolipoproteins APOB100, APOD, APOE, APOF, APOL1, APOM; serum amyloid A2, serum amyloid P component) (Fig. 1.B). Since 100% depletion of high abundance proteins is practically impossible to achieve, relative quantitation from label free proteomics investigations should be viewed with caution. Validation was hereby provided for TTR via LC-SRM, suggesting that, since depletion protocols were the same for both male and female PLT supernatants, male donors might have constitutively higher TTR levels, that are only partially depleted, or forms of the protein missing the depletion epitope altogether. Male-donor PLT supernatants were also characterized by higher levels of extracellular matrix (ECM) proteins, including cartilage acidic protein 1, tenascin (TNC), factor X, and α -hemoglobin and β -hemoglobin subunits (as confirmed by targeted LC-SRM assays).

3.3. Coagulation and inflammation

Storage led to decreased levels of pro-coagulation factors (GO:0009611), such as angiotensinogen, fibronectin, gelsolin, plasminogen, but also of anti-coagulation factors (e.g. alpha 2-antiplasmin, antithrombin-III, Inter-alpha trypsin inhibitor heavy chain H4, vitamin K-dependent protein S – PROS1, validated through LC-SRM – Fig. 2.A). At the same time, male-donor PLT supernatants were characterized by higher levels of coagulation factors IX, X, XI, XII, prothrombin, heparin cofactor 2, gelsolin isoform 2, kallistatin, though they tended to decrease in a storage-dependent fashion (Fig. 3.B). On the other hand, PLT supernatants from female donors were characterized by constitutively and storage duration independent levels of alpha-2 macroglobulin (confirmed by LC-SRM – Fig. 6.B), coagulation factor XIII B, fibrinogen beta chain (validated against stable isotope labeled standards – Fig. 6.B), plasma kallikrein, and serine-protease inhibitors (SERPINs, alpha trypsin inhibitor heavy chain H1, H3 isoform 2, H4, isoform 2 – Fig. 1.A), or storage-dependent increases in fibrinogen alpha and gamma chains and plasminogen activator inhibitor (also increasing in male donor PLT supernatants, though to a lesser extent – Fig. 4.A).

3.4. Complement system and inflammation

There was a storage-dependent and gender-independent decrease in the levels of complement components, classical pathway (GO:0006958-C1s, C5, C6, C7, C8, C9 – Fig. 2.A). On the other hand, PLT supernatants from male donors were constitutively enriched with components of the alternative complement pathway (Complement factor D, H-related protein 1, 2 and 4 isoform 1). The alternative complement pathway is responsive to microbial infection activation. Therefore, these results should be interpreted together with the observed constitutive (Fig. 1.B) or storage-dependent (e.g. lysozyme, lipopolysaccharide binding protein – Fig. 4.B) up-regulation of antimicrobial proteins and peptides in the supernatants of apheresis PLTs from male donor. However, the late effector complement component C3, which is at the crossroads between classical and alternative complement system pathways, was found to increase in a gender-independent storage-dependent fashion

(Fig. 3.B), despite being one of the targets of depletion via affinity columns. Analogously, complement component 4B (another late player in the complement system activation cascade) increased in a storage-dependent fashion, especially in the male group (Fig. 3.B), while properdin, a positive regulator of the alternate pathway, was increased in the female group (Fig. 3.A), suggesting a progressive activation of this pathway in the supernatant of stored PLTs. (Fig. 3.B). Moreover, in male donors storage-dependent increases were observed in the supernatant levels of the isoform 4 of latent transforming growth-factor beta (Fig. 4.B). In line with this, vasorin, a potential TGFB-signaling inhibitor, was found to decrease in a storage-dependent fashion (Fig. 2.A). Storage-dependent increases in cytokine components were hereby observed as well (platelet factor 4, platelet basic protein – Fig. 2.B).

3.5. Apoptosis

Decreases in gelsolin supernatants levels were observed and were independent of donor gender (Fig. 1.A). Consistently, other proteins potentially involved in apoptosis (GO: 0043065 – Supplementary Table 1) were less abundant in day 5 supernatants, including, tumor necrosis factor alpha receptor family member 1A, other than the previously mentioned complement components C6 and C9 (Fig. 2.A).

3.6. Cell adhesion

Storage promoted a broad deregulation of extra-cellular matrix (ECM- GO:0007596) and structural proteins (GO:0003779). Storage and gender-independent decreases were observed in the levels of lumican, isoform F of proteoglycan 4, isoform 1 of vascular cell adhesion protein 1, isoform 3 of muscular LMNA-interacting protein (Fig. 2.A). Gender-specific storage-dependent decreases were observed as well, such as in the case of plastin-2 (female donors – Fig. 3.A) or vitronectin (male donors – Fig. 3.B). However, storage-dependent up-regulation of other components were observed as well, including cofilin 1, 14-3-3 protein zeta/delta, actin-related protein 2/3 complex subunit 2, tropomyosin alpha-4 and 6, tubulin alpha chain, profilin-1, talin-1, platelet glycoprotein V (validated – Fig. 6.B), multimerin 2, thrombospondin 1 (both in label-free and targeted MS assays – Fig. 6.B), vinculin (Fig. 2.B). Gender-specific storage dependent increases were observed as well, both in female donors (collagen alpha-1 (XVIII), coronin 1C, actin-related protein 2, moesin, non-muscle isoform of myosin light polypeptide 6, protocadherin-8, tropomyosin isoform, ankyrin 3, synaptotagmin-7, p-selectin, metalloproteinase inhibitor 1, fermitin family homolog 3, pleckstrin, alpha-actinin 1 – Fig. 4.A) and male donors (isoform 1 of multimerin, 14-3-3 protein eta and theta, fibronectin, actin-related protein 2/3 complex subunit 4, nidogeni-1, tubulin beta chain – Fig. 4.B). Increased storage-dependent levels of “cell free” platelet glycoprotein Ib and IIb alpha in female and male donors, respectively (Fig. 4.A and B), might be more or less directly related to the previously reported structural remodeling via integrin α IIb β 3 signaling pathways [14].

3.7. Metabolism and oxidative stress

Storage resulted in the progressive supernatant accumulation of proteins involved in cell energy and redox-metabolism (GO:0006096, IPR010987), both in a gender-independent (Fig. 2.B) or dependent (Fig. 4.A and B) fashion. The release of these enzymes might stem

either from cell lysis, resulting in subsequent release in the supernatant of intracellular products, or from vesiculation mechanisms.

The list of proteins in this group includes glycolytic enzymes (fructose biphosphate aldolase, triosephosphate isomerase, glyceraldehyde 3-phosphate dehydrogenase, phosphoglycerate mutase 1, lactate dehydrogenase A) and anti-oxidant enzymes (glutathione S-transferase omega-1 and P, peroxiredoxin 6) in all donors (Fig. 2.B). Female-specific storage-dependent increases in metabolic enzymes include nucleoside diphosphate kinase A, phosphoglycerate kinase, transaldolase, sphingomyelin phosphodiesterase 2 and L-lactate dehydrogenase B (Fig. 4.A). On the other hand, male donors showed late storage increases in creatine kinase M, nucleoside diphosphate kinase B and pyruvate kinase M1/M2 (Fig. 4.B).

Storage corresponded to a decrease in the levels of ceruloplasmin (Fig. 2.A), a copper protein involved in iron metabolism, and an increase of antioxidant enzymes other than peroxiredoxins and GSH-transferases, including superoxide dismutase [Cu-Zn] in female donors (Fig. 4.A) and protein DJ-1 in the male group (Fig. 4.B).

4. Discussion

PLT concentrates can be obtained either from pooling of whole blood-derived buffy coats from multiple donors, or apheresis (also referred to as platepheresis) from a single donor. Differential storage lesions in the cell fraction of both blood-derived therapeutics have been extensively documented in the literature [11–14]. However, the proteomics lesions accumulating in the supernatants of stored PLTs have been so far limited to buffy coat concentrates [29,30], while proteome changes in apheresis-derived PLT supernatants have only focused on platelet factor 4 and β -thromboglobulin [20].

In their pioneering study, Glenister and colleagues [29] exploited 2D gel electrophoresis (GE) maps of buffy coat-derived PLT supernatant proteins to highlight changes to major plasma proteins. PLT-derived proteins were also identified, including tremlike transcript 1 and integrin-linked kinase, which may influence PLT–endothelium interactions. Moreover, the Authors detected increased storage-dependent accumulation in the supernatants of PLT derived cytokines including brain-derived neurotrophic factor (BDNF), CXCL7 (validated through LC-SRM – Fig. 6.B), epidermal growth factor, PLT-derived growth factor (PDGF), and CCL5 [29].

The biological relevance of PLT protein releasates has been previously documented to mediate PLT-triggered coagulation, inflammatory and acute phase responses [11]. However, the presence of plasma in the supernatant additive solution hampers the detection of low abundance proteins, and thus prevents any in-depth investigation of quantitative changes of supernatant proteins during storage in the blood bank. In a recent study, Egidi and colleagues have tackled this issue by performing initial selective enrichment of the buffy coat PLT supernatant low abundance proteome via combinatorial hexapeptide ligand libraries, followed by 2D-GE analyses [30].

In the present study, we performed a preliminary depletion of the most abundant 14 plasma proteins from apheresis PLT supernatants, coupled with 1D-SDS-PAGE/nanoLC-MS/MS

analyses, a strategy that has been previously described in successful plasma proteomics investigations as a viable solution to cope with the widespread dynamic range of concentrations of proteins from this biological fluid [5,25]. This strategy favored an increased coverage of the PLT supernatant proteome in comparison to previous studies [11,20,29,30], enabling detection of 503 distinct proteins in PLT supernatants. Additionally, validation using a targeted MS-based approach confirmed quantitative trends determined through label-free assays for a subset of proteins showing significant fold-change variations in a gender or storage-dependent fashion.

4.1. Gender-specificity of PLT supernatants

Apheresis PCs are resuspended in donors' plasma. Concerns have recently arose about gender-related differences in PLT biology [32,33] and plasma proteomes [25]. The significance of gender-specific differences in the PLT proteome has previously been anticipated, as a likely contributing factor that could impact gender-influenced cardiovascular disease profiling, potentially resulting from differences in individual capacity of protein translation [6]. We previously documented gender-related plasma proteome differences [25] and were thus not surprised by differences in PC supernatant profiles from male and female donors.

Many gender-related specific proteins were identified in stored units both at day1 and at the end of the storage period, such as pregnancy zone protein, a protein associated with late-pregnancy sera from women donors [29] but also found in non-pregnant women [34]. Functional classification of gender and storage-dependent proteomes included proteins involved in coagulation, complement and inflammation, apoptosis, PLT activation or energy and redox metabolism-associated proteins, as detailed below. Among the peculiar gender-specific proteins we observed, hemoglobin subunits alpha and beta were only detected in platelet supernatants from male donors. Although this result might be affected by hemolysis byproduct contamination, it is worth noting that mature PLTs harbor residual mRNAs to sustain limited *de novo* protein synthesis [6], and hemoglobin mRNAs have been identified in the mature PLT transcriptome [35].

4.2. Coagulation and inflammation

From a biological standpoint, it is worth recalling that the main purpose of issuing PCs (both the supernatant and cell fraction) is to restore hemostasis by improving coagulation time and efficiency. In this view, it is interesting to note that storage and gender affected proteins involved in coagulation cascades. PLT storage promoted a general decrease in hemostatic proteins, while male PLT supernatants were richer in coagulation factors from IX to XII, and female counterparts showed higher levels of alpha-2 macroglobulin (as confirmed both through label-free and targeted MS approaches) and SERPINS. Gender-specific levels of proteins related to hemostasis might suggest that PC from male and female donors might differently perform hemostatic functions upon transfusion, thus suggesting the necessity for further functional experiments.

4.3. Complement system and inflammation

Most of the components of the classical complement system decreased in all PCs. However, male donor PC supernatants were more enriched with alternative pathway complement components. It can be noted that the complement system plays a key role in immunity and inflammation, while previous studies had reported the storage dependent accumulation in the PLT releasates of pro-inflammatory mediators and cytokines, such as PLT factor 4 (PF4 – hereby confirmed through the LC-SRM approach – Fig. 6) and β -thromboglobulin (β -TG) [20], or BDNF, CCL5, PDGF and clusterin (a complement-mediated lysis inhibitor, apparently higher in abundance in male donor supernatants – Fig. 6.A and B), TLT-1 (having a role in PLT adhesion) and ILK (aggregation and adhesion to damaged endothelium) [29]. Cytokine expression can be modulated by tumor necrosis factor alpha and transforming growth factor beta (TGFB) [36], the latter appearing to increase in a storage-dependent gender-dependent fashion in PLT male supernatants.

4.4. Apoptosis

Previous studies on PLT storage had shown a storage-dependent alteration of intracellular gelsolin levels [12–14], a protein that was associated with an apoptosis-like event underlying PLT storage, together with increased beta-actin fragmentation and septin 2 deregulation. Storage-dependent decreases in gelsolin supernatants levels were detected, and were independent of donor gender. Gelsolin-depletion/ alteration had previously been reported in post shock mesenteric lymph in trauma models, whereby gelsolin is deemed to be a marker of apoptosis [37]. Gender-independent, storage-dependent decreases of gelsolin and other apoptosis markers in the supernatants were observed, and might be to some extent related to the previously reported storage-dependent increase in the intracellular level of these proteins [12–14].

4.5. Cell adhesion

Previous investigations on PLT storage have highlighted a progressive alteration of structural and cell adhesion proteins, utterly promoting morphological score impairment and altered functionality of long-stored PLTs [11–13]. Structural, signaling or focal adhesion proteins (e.g. beta-actin, coronin 1A, tropomyosin alpha-4 chain, 14-3-3 proteins, plectrostrin, α -actinin, moesin, vinculin, fermitin family homolog 3 (kindlin-3), and filamin A) had been found to be deregulated early upon storage in an integrin α IIb β 3 signaling pathway-mediated fashion [14]. In the present study we confirm a broad deregulation of ECM and structural proteins (e.g. lumican, isoform F of proteoglycan 4, isoform 1 of vascular cell adhesion protein 1, isoform 3 of muscular LMNA-interacting protein), while gender-specific storage-dependent decreases were observed in the levels of plastin-2 (female donors) and vitronectin (male donors). At the same time, storage promoted increases in the abundance of serglycin (SRGN – Fig. 6.A and B), a protein involved in MMP2 processing and thus, indirectly, in ECM remodeling [38]. Storage-dependent increases of other adhesion proteins might indirectly mirror storage-triggered gender-specific cascades, resulting in the progressive loss of PLT structural integrity and increased PLT activation (focal adhesion, ECM remodeling), with PLTs from female donors apparently being more sensitive to this phenomenon. Since structural proteins are strictly tied to PLT physiology and activation,

gender and storage-dependent alterations of this class of proteins might mirror impairments of PLT function.

4.6. Metabolism and oxidative stress

PLT lysis or granule releases might be responsible for the observed accumulation of metabolism and oxidative stress-related proteins in the supernatants, especially in units from female donors. In the extracellular environment, these enzymes might either be inactive or preserve their activity, provided the absence of regulatory post-translational modifications and buffering of the pH drop associated with PLT storage [1–3]. Alternatively, extracellular enzymes might show as of yet undisclosed or underinvestigated catalytic functions, a typical phenomenon associated to the so-called “moonlighting proteins” [39]. Two examples of this phenomenon might be embodied by peroxiredoxins and glyceraldehyde 3-phosphate dehydrogenase (antioxidant and glycolytic enzymes, respectively), also playing a role in iron transport [40] and lipid metabolism [41], thereby mediating pro-oxidant and inflammatory responses [39]. Consistently, increased levels of oxidative-stress-related proteins were observed in day 5 PC supernatants, such as ceruloplasmin, peroxiredoxins and GSH-transferases, other than superoxide dismutase [Cu-Zn] (female donors) and DJ-1 (male donors).

5. Conclusion

The present study was designed to investigate storage and gender-specific proteomic alterations to the supernatants of PCs from male and female donors. Despite the exploratory nature of this study, addressing a limited cohort of donors without distinction of biological variables other than gender (e.g. smoking habits, age, etc.), we hereby observed a storage-dependent impairment of extracellular blood coagulation mediators, together with storage and gender-specific alterations in the levels of pro-inflammatory complement components and cytokines. In order to partially cope with intrinsic technical caveats deriving from label-free quantitative approaches and the limited number of technical and biological replicates, we performed a validation on a subset of proteins through targeted LC-SRM assays against QConCAT generated standard peptides. Both approaches highlighted the deregulation of structural proteins and increased supernatant levels of ECM and focal adhesion proteins are likely suggestive of an activated state of long-stored PLTs, especially from female donors. In addition, the observed increase in storage-dependent accumulation of energy and redox metabolic enzymes might result from cell lysis or granule release. The released proteins (especially enzymes) might still exert their normal catabolic activity, or rather perform alternative “moonlighting” biological functions [38].

Taken together, the observed results indicate gender specific traits in stored PLT supernatants, with the supernatants from female donors being characterized by a more sustained increase in the levels of several proteins, which might represent a further burden in PLT activation, ECM remodeling and focal adhesion components. Future functional studies will determine whether such a biological signature might correlate with untoward effects observed in recipients receiving transfusion of prestorage-leukoreduced stored PLT concentrates.

Finally, it should be noted that countries such as France and the United Kingdom do not allow the collection of platelets from women, due to the increased risk of TRALI. This risk is thought to be related to high anti-HLA or anti-neutrophil antibodies in plasma from parous women [42]. If confirmed, the presented results should help further inform policies regarding sex selection of PLT donors worldwide.

Supplementary Material

Refer to Web version on PubMed Central for supplementary material.

Acknowledgments

Financial Support: This work was supported in part by grants from the National Institutes of Health, National Institute of General Medical Sciences grants: T32-GM008315 and P50-GM049222, National Center for Research Resources (S10RR023015), and by NIH/NCATS Colorado CTSA (UL1 TR001082).

References

1. Devine DV, Serrano K. The platelet storage lesion. *Clin Lab Med.* 2010; 30:475–87. [PubMed: 20513565]
2. Ohto H, Nollet KE. Overview on platelet preservation: better controls over storage lesion. *Transfus Apher Sci.* 2011; 44:321–5. [PubMed: 21507724]
3. Shrivastava M. The platelet storage lesion. *Transfus Apher Sci.* 2009; 41:105–13. [PubMed: 19683964]
4. Goodrich RP, Li J, Pieters H, Crookes R, Roodt J, Heyns Adu P. Correlation of in vitro platelet quality measurements with in vivo platelet viability in human subjects. *Vox Sang.* 2006; 90:279–85. [PubMed: 16635070]
5. Liumbruno G, D'Alessandro A, Grazzini G, Zolla L. Blood-related proteomics. *J Proteomics.* 2010; 73(3):483–507. [PubMed: 19567275]
6. Schubert P, Devine DV. De novo protein synthesis in mature platelets: a consideration for transfusion medicine. *Vox Sang.* 2010; 99:112–22. [PubMed: 20345520]
7. Burkhart JM, Gambaryan S, Watson SP, Jurk K, Walter U, Sickmann A, et al. What can proteomics tell us about platelets? *Circ Res.* 2014; 114(7):1204–19. [PubMed: 24677239]
8. Senis Y, Garcia A. Platelet proteomics: state of the art and future perspective. *Methods Mol Biol.* 2012; 788:367–99. [PubMed: 22130719]
9. Prudent M, D'Alessandro A, Cazenave JP, Devine DV, Gachet C, Greinacher A, et al. Proteome changes in platelets after pathogen inactivation—an interlaboratory consensus. *Transfus Med Rev.* 2014; 28(2):72–83. [PubMed: 24685438]
10. Zufferey A, Fontana P, Reny JL, Noll S, Sanchez JC. Platelet proteomics. *Mass Spectrom Rev.* 2012; 31:331–51. [PubMed: 22009795]
11. Coppinger JA, Cagney G, Toomey S, Kislinger T, Belton O, McRedmond JP, et al. Characterization of the proteins released from activated platelets leads to localization of novel platelet proteins in atherosclerotic lesions. *Blood.* 2004; 103:2096–104. [PubMed: 14630798]
12. Thon JN, Schubert P, Duguay M, Serrano K, Lin S, Kast J, et al. Comprehensive proteomic analysis of protein changes during platelet storage requires complementary proteomic approaches. *Transfusion.* 2008; 48:425–35. [PubMed: 18067510]
13. Thiele T, Steil L, Gebhard S, Scharf C, Hammer E, Brigulla M, et al. Profiling of alterations in platelet proteins during storage of platelet concentrates. *Transfusion.* 2007; 47:1221–33. [PubMed: 17581157]
14. Thiele T, Iuga C, Janetzky S, Schwertz H, Gesell Salazar M, Furl B, et al. Early storage lesions in apheresis platelets are induced by the activation of the integrin α IIb β (3) and focal adhesion signaling pathways. *J Proteomics.* 2012; 76:297–315. [PubMed: 22634086]

15. Prudent M, Crettaz D, Delobel J, Tissot JD, Lion N. Proteomic analysis of Intercept-treated platelets. *J Proteomics*. 2012; 76:316–28. [PubMed: 22813878]
16. Marrocco C, D'Alessandro A, Girelli G, Zolla L. Proteomic analysis of platelets treated with gamma irradiation versus a commercial photochemical pathogen reduction technology. *Transfusion*. 2013; 53:1808–20. [PubMed: 23305084]
17. Schubert P, Culibrk B, Coupland D, Scammell K, Gyongyossy-Issa M, Devine DV. Riboflavin and ultraviolet light treatment potentiates vasodilator-stimulated phosphoprotein Ser-239 phosphorylation in platelet concentrates during storage. *Transfusion*. 2012; 52:397–408. [PubMed: 21827504]
18. Prudent M, Sonogo G, Abonnenc M, Tissot JD, Lion N. LC-MS/MS analysis and comparison of oxidative damages on peptides induced by pathogen reduction technologies for platelets. *J Am Soc Mass Spectrom*. 2014; 25(4):651–61. [PubMed: 24470194]
19. Harr JN, Moore EE, Chin TL, Gonzalez E, Wohlauser M, Banerjee A, et al. Platelets are dominant contributors to hypercoagulability after injury. *J Trauma Acute Care Surg*. 2013; 74(3):756–62. [PubMed: 23425732]
20. Wurtz V, Hechler B, Ohlmann P, Isola H, Schaeffer-Reiss C, Cazenave JP, et al. Identification of platelet factor 4 and β -thromboglobulin by profiling and liquid chromatography tandem mass spectrometry of supernatant peptides in stored apheresis and buffy-coat platelet concentrates. *Transfusion*. 2007; 47:1099–100. [PubMed: 17524104]
21. Silliman CC, Bjornsen AJ, Wyman TH, Kehler M, Allard J, Bieber S, et al. Plasma and lipids from stored platelets cause acute lung injury in an animal model. *Transfusion*. 2003; 43(5):633–40. [PubMed: 12702186]
22. Kanter J, Khan SY, Kelher M, Gore L, Silliman CC. Oncogenic and angiogenic growth factors accumulate during routine storage of apheresis platelet concentrates. *Clin Cancer Res*. 2008; 14(12):3942–7. [PubMed: 18559616]
23. Dineen SP, Roland CL, Toombs JE, Kehler M, Silliman CC, Brekken RA, et al. The acellular fraction of stored platelets promotes tumor cell invasion. *J Surg Res*. 2009; 153(1):132–7. [PubMed: 18541268]
24. Coppinger JA, Cagney G, Toomey S, Kislinger T, Belton O, McRedmond JP, et al. Characterization of the proteins released from activated platelets leads to localization of novel platelet proteins in human atherosclerotic lesions. *Blood*. 2004; 103(6):2096–104. [PubMed: 14630798]
25. Silliman CC, Dziewiatkowska M, Moore EE, Kehler M, Banerjee A, Liang X, et al. Proteomic analyses of human plasma: Venus versus Mars. *Transfusion*. 2012; 52(2):417–24. [PubMed: 21880043]
26. Pratt JM, Simpson DM, Doherty MK, Rivers J, Gaskell SJ, Beynon RJ. Multiplexed absolute quantification for proteomics using concatenated signature peptides encoded by QconCAT genes. *Nat Protoc*. 2006; 1(2):1029–43. [PubMed: 17406340]
27. Dziewiatkowska M, Hill R, Hansen KC. GeLC-MS/MS analysis of complex protein mixtures. *Methods Mol Biol*. 2014; 1156:53–66. [PubMed: 24791981]
28. MacLean B, Tomazela DM, Shulman N, Chambers M, Finney GL, Frewen B, et al. Skyline: an open source document editor for creating and analyzing targeted proteomics experiments. *Bioinformatics*. 2010; 26(7):966–8. [PubMed: 20147306]
29. Glenister KM, Payne KA, Sparrow RL. Proteomic analysis of supernatant from pooled buffy-coat platelet concentrates throughout 7-day storage. *Transfusion*. 2008; 48:99–107. [PubMed: 17894789]
30. Egidi MG, Rinalducci S, Marrocco C, Vaglio S, Zolla L. Proteomic analysis of plasma derived from platelet buffy coats during storage at room temperature. An application of ProteoMiner (TM) technology. *Platelets*. 2011; 22:252–69. [PubMed: 21405958]
31. Skornicka EL, Kiyatkina N, Weber MC, Tykocinski ML, Koo PH. Pregnancy zone protein is a carrier and modulator of placental protein-14 in T-cell growth and cytokine production. *Cell Immunol*. 2004; 232(1–2):144–56. [PubMed: 15882859]
32. Breet NJ, Sluman MA, van Berkel MA, van Wekum JW, Bouman HJ, Harmsze AM, et al. Effect of gender difference on platelet reactivity. *Neth Heart J*. 2011; 19(11):451–7. [PubMed: 21901505]

33. Biino G, Santimone I, Minelli C, Sorice R, Frongia B, Traglia M, et al. Age- and sex-related variations in platelet count in Italy: a proposal of reference ranges based on 40987 subjects' data. *PLoS One*. 2013; 8(1):e54289. [PubMed: 23382888]
34. Petersen CM, Jensen PH, Bukh A, Sunde L, Lamm LU, Ingerslev J. Pregnancy zone protein: a re-evaluation of serum levels in healthy women and in women suffering from breast cancer or trophoblastic disease. *Scand J Clin Lab Invest*. 1990; 50(5):479–85. [PubMed: 1700464]
35. Gnatenko DV, Dunn JJ, McCorkle SR, Weissmann D, Perrotta PL, Bahou WF. Transcript profiling of human platelets using microarray and serial analysis of gene expression. *Blood*. 2003; 101:2285–93. [PubMed: 12433680]
36. Silberstein FC, De Simone R, Levi G, Aloisi F. Cytokinereregulated expression of platelet-derived growth factor gene and protein in cultured human astrocytes. *J Neurochem*. 1996; 66(4):1409–17. [PubMed: 8627292]
37. Dziedziatowska M, Wohlaer MV, Moore EE, Damle S, Peltz E, Campsen J, et al. Proteomic analysis of human mesenteric lymph. *Shock*. 2011; 35(4):331–8. [PubMed: 21192285]
38. Lundequist A, Abrink M, Pejler G. Mast cell-dependent activation of pro matrix metalloproteinase 2: A role for serglycin proteoglycan-dependent mast cell proteases. *Biol Chem*. 2006; 387(10–11): 1513–9. [PubMed: 17081126]
39. Jeffery CJ. Moonlighting proteins: old proteins learning new tricks. *Trends Genet*. 2003; 19(8): 415–7. [PubMed: 12902157]
40. Polati R, Castagna A, Bossi AM, Alberio T, De Domenico I, Kaplan J, et al. Murine macrophages response to iron. *J Proteomics*. 2012; 76:10–27. [PubMed: 22835775]
41. Chen JW, Dodia C, Feinstein SI, Jain MK, Fisher AB. 1-Cys peroxiredoxin, a bifunctional enzyme with glutathion peroxidase and phospholipase A2 activities. *J Biol Chem*. 2000; 275:28421–7. [PubMed: 10893423]
42. Gajic O, Yilmaz M, Iscimen R, Kor DJ, Winters JL, Moore SB, et al. Transfusion from male-only versus female donors in critically ill recipients of high plasma volume components. *Crit Care Med*. 2007; 35(7):1645–8. [PubMed: 17522583]

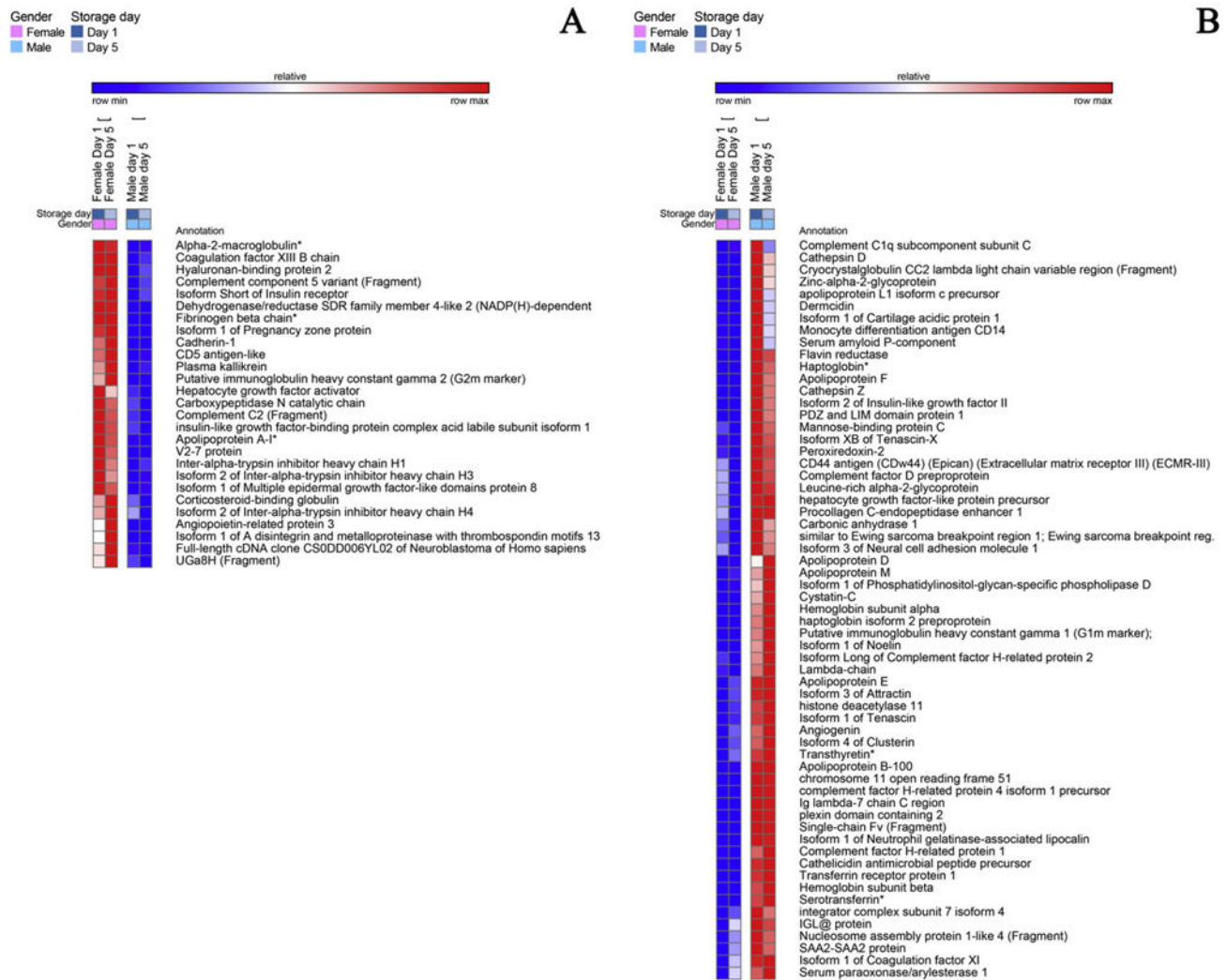


Fig. 1. A detail of heat maps showing quantitative dynamic proteomics changes in apheresis platelet supernatants from male and female donors at storage day 1 and 5. Proteins constitutively higher (storage-independent gender-dependent) in female (A) and male (B) donors are mapped.

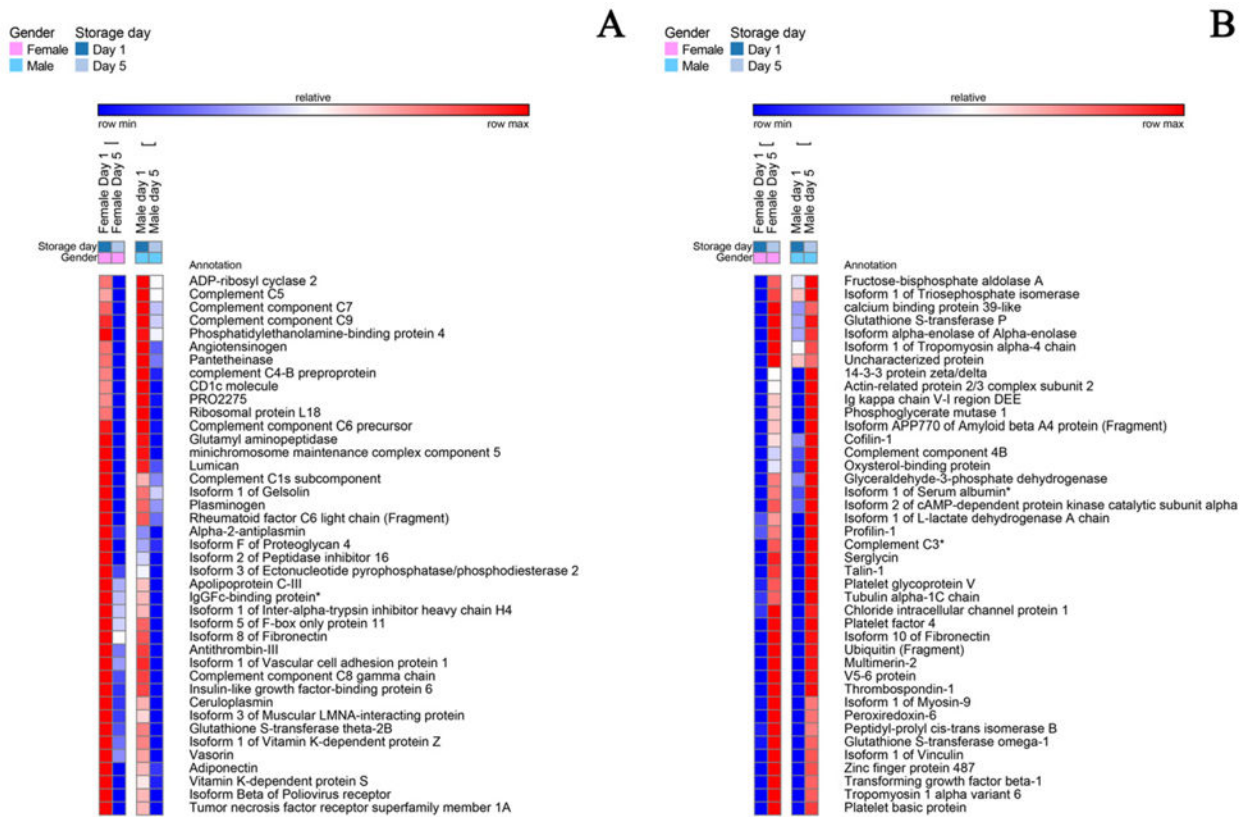


Fig. 2. A detail of heat maps showing quantitative dynamic proteomics changes in apheresis platelet supernatants from male and female donors at storage day 1 and 5. Proteins decreasing (A) or increasing (B) in a storage-dependent gender-independent fashion in female and male donors are mapped.

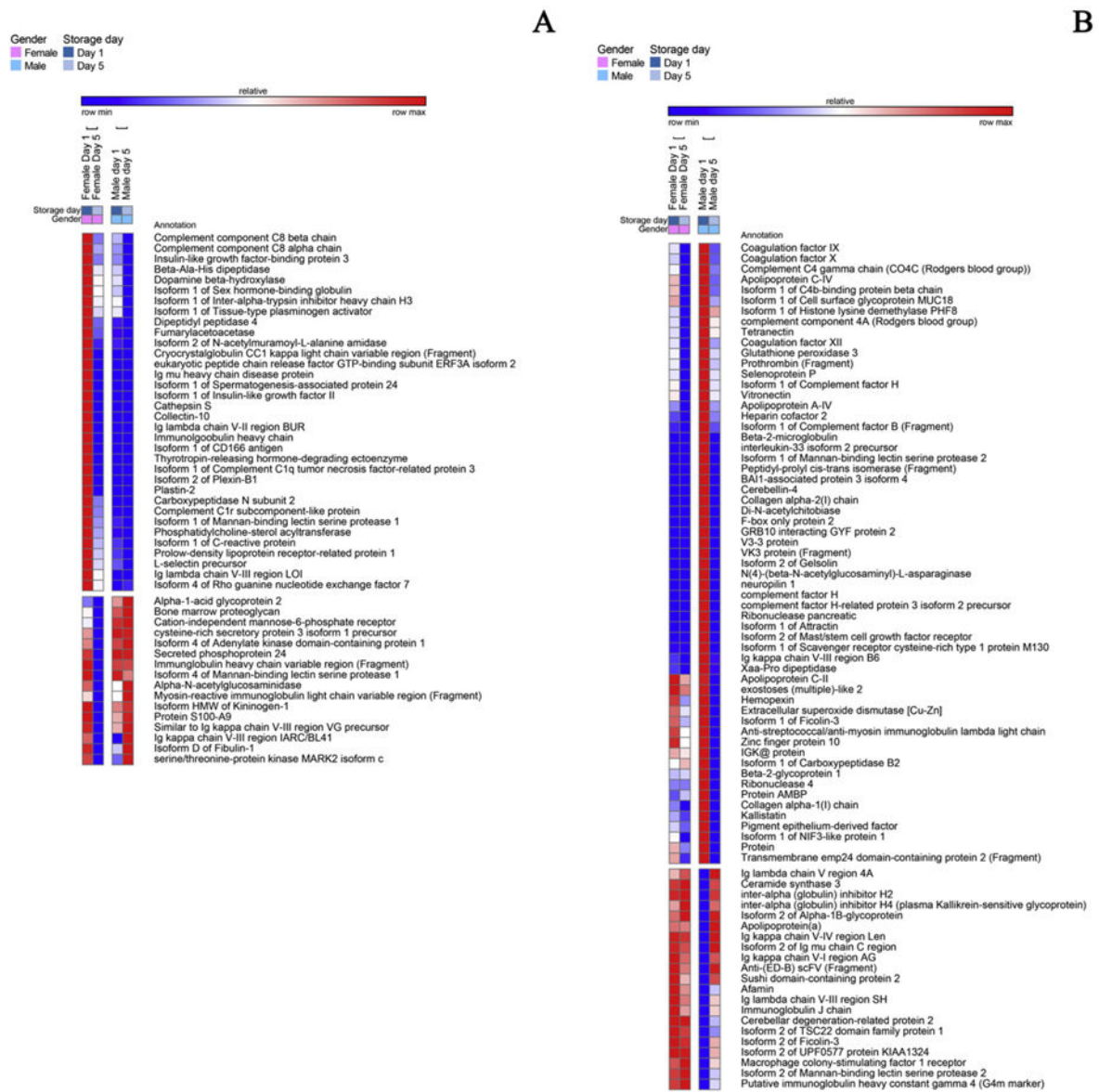


Fig. 3. A detail of heat maps showing quantitative dynamic proteomics changes in apheresis platelet supernatants from male and female donors at storage day 1 and 5. Proteins decreasing either in female (A) or male donors (B) in a storage and gender-dependent fashion are mapped.

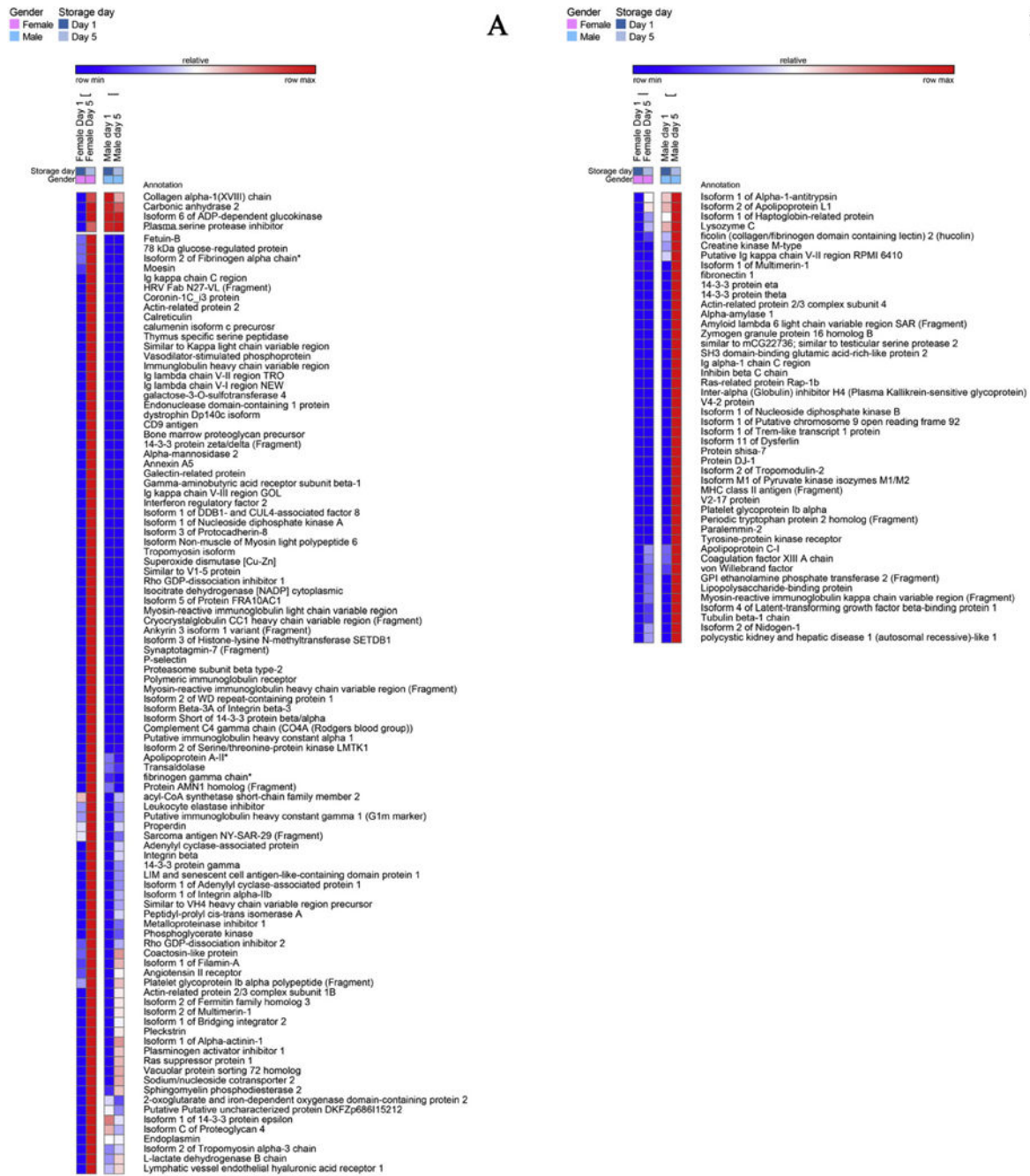


Fig. 4. A detail of heat maps showing quantitative dynamic proteomics changes in apheresis platelet supernatants from male and female donors at storage day 1 and 5. Proteins increasing either in female (A) or male donors (B) in a storage and gender-dependent fashion are mapped.

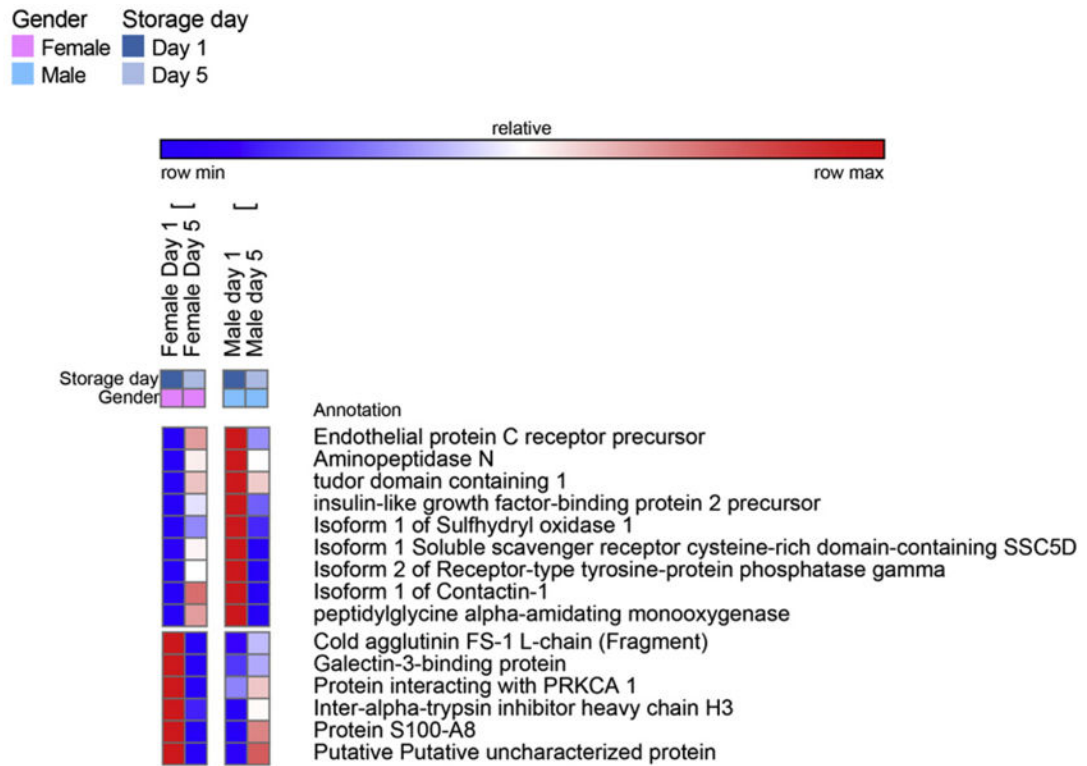


Fig. 5. A detail of heat maps showing quantitative dynamic proteomics changes in apheresis platelet supernatants from male and female donors at storage day 1 and 5. Proteins showing opposite gender-dependent trends in a storage-dependent fashion are mapped.

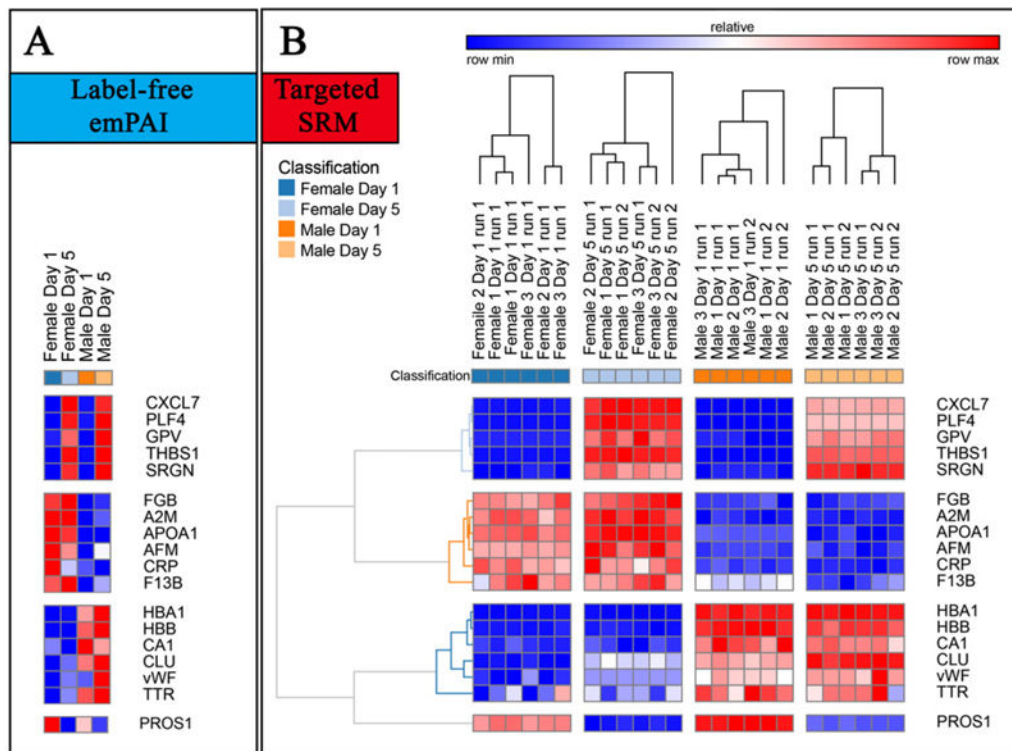


Fig. 6. In A, a detail of a subset of proteins from apheresis platelet supernatants showing significant quantitative variations with respect to storage duration (top and bottom clusters), gender (second and third cluster from the top), as determined through label-free mass spectrometry-based approaches. In B, heat maps represent quantitative fluctuations of the very same proteins, as determined through targeted approaches based upon LC-SRM against labeled QConCAT standards.

Table 1

Platelet supernatants from female or male donors assayed as storage day 1 or 5.

#	Identified Proteins (503)	IPi N.	MW	Female day 1	Female day 5	Male day 1	Male day 5	
1	Apolipoprotein B-100	IPi00022229	516 kDa	4724	5014	7081	7252	
2	Alpha-2-macroglobulin*	IPi00478003	163 kDa	6798	6802	5174	5477	
3	Isoform 1 of Serum albumin*	IPi00745872	69 kDa	2934	4536	3329	5160	
4	Ceruloplasmin	IPi00017601	122 kDa	2870	2427	2765	2435	
5	Hemopexin	IPi00022488	52 kDa	2170	1972	2293	1876	
6	Serotransferrin*	IPi00022463	77 kDa	1361	1399	2437	2662	
7	Isoform 1 of Complement factor H	IPi00029739	139 kDa	1872	1701	2117	1936	
8	Isoform 1 of Fibrinogen alpha chain*	IPi00021885	95 kDa	1691	1688	1571	1438	
9	Isoform 8 of Fibrinectin	IPi00339228	253 kDa	2069	1483	1932	896	
10	Vitamin D-binding protein isoform 3 precursor	IPi00968027	55 kDa	1606	1491	1455	1184	
11	Inter-alpha-trypsin inhibitor heavy chain H1	IPi00292530	101 kDa	1463	1470	1426	1465	
12	PRO2275	IPi00305457	135 kDa	1264	1104	1371	1145	
13	Isoform 1 of Tissue-type plasminogen activator	IPi00019590	217 kDa	1398	1212	1238	1077	
14	Complement C3*	IPi00783987	187 kDa	882	1359	914	1490	
15	Fibrinogen beta chain*	IPi00298497	56 kDa	1116	1138	923	944	
16	complement C4-B preproprotein	IPi00418163	193 kDa	1225	795	1414	860	
17	Plasminogen	IPi00019580	91 kDa	992	831	987	910	
18	Isoform Gamma-A of Fibrinogen gamma chain*	IPi00219713	49 kDa	868	1007	911	867	
19	Protein	IPi001025666	72 kDa	887	853	970	831	
20	Complement component 4B	IPi00887154	193 kDa	621	863	728	1223	
21	Histidine-rich glycoprotein	IPi00022371	60 kDa	808	790	747	693	
22	Antithrombin-III	IPi00032179	53 kDa	809	662	809	629	
23	Alpha-1-acid glycoprotein 1*	IPi00022429	140 kDa	820	806	748	654	
24	Transthyretin*	IPi00022432	16 kDa	601	689	874	925	
25	Prothrombin (Fragment)	IPi00019568	70 kDa	764	672	908	787	
26	complement component 4A (Rodgers blood group)	IPi00643525	193 kDa	639	512	832	699	
27	similar to Ewing sarcoma breakpoint region 1; Ewing sarcoma breakpoint reg. 1	IPi00877697	92 kDa	586	535	816	746	
28	Inter-alpha (globulin) inhibitor H4 (plasma kallikrein-sensitive glycoprotein)	IPi00944960	104 kDa	741	795	694	790	
29	Cerebellar degeneration-related protein 2	IPi00009862	315 kDa	632	643	428	525	
30	Complement C5	IPi00032291	188 kDa	577	369	696	543	
31	Isoform Short of Insulin receptor	IPi00220325	231 kDa	690	719	530	579	
32	Isoform 1 of Alpha-1-antitrypsin	IPi00553177	47 kDa	335	471	502	619	
33	Apolipoprotein A-IV	IPi00304273	45 kDa	499	452	637	528	
34	C4b-binding protein alpha chain	IPi00021727	67 kDa	511	477	430	393	
35	Haptoglobin*	IPi00641737	45 kDa	186	198	799	676	
36	Transmembrane emp24 domain-containing protein 2 (Fragment)	IPi01012491	74 kDa	457	391	523	379	
37	Isoform 1 of Gelsolin	IPi00026314	86 kDa	438	413	444	439	
38	Isoform 1 of Inter-alpha-trypsin inhibitor heavy chain H4	IPi00896419	103 kDa	545	434	490	366	
39	Isoform 1 of Alpha-1B-glycoprotein	IPi00022895	54 kDa	322	325	327	292	
40	Vitronectin	IPi00298971	54 kDa	298	255	349	306	
41	Zinc finger protein 10	IPi00796989	130 kDa	334	302	350	265	
42	Full-length cDNA clone CS0DD006YL02 of Neuroblastoma of Homo sapiens	IPi00479708	41 kDa	404	537	287	258	
43	Glutathione S-transferase theta-2B	IPi00956139	207 kDa	372	305	361	299	
44	Protein AMBP	IPi00022426	39 kDa	333	351	391	336	
45	Complement C4 gamma chain (CO4C (Rodgers blood group))	IPi00892547	193 kDa	364	78	691	259	
46	Angiotensinogen	IPi00032220	53 kDa	428	359	463	389	
47	Beta-2-glycoprotein 1	IPi00298828	38 kDa	305	314	371	282	
48	Isoform 1 of Histone lysine demethylase PHF8	IPi00480187	200 kDa	330	187	536	426	
49	Heparin cofactor 2	IPi00879573	57 kDa	240	220	345	264	
50	Complement component C6 precursor	IPi00879709	106 kDa	293	255	304	264	
51	Complement C1s subcomponent	IPi00017696	77 kDa	327	276	317	300	
52	Afarmin	IPi00019943	69 kDa	294	263	180	235	
53	Apolipoprotein A-I*	IPi00021841	31 kDa	268	264	227	227	
54	Zinc-alpha-2-glycoprotein	IPi00166729	62 kDa	196	191	368	299	
55	Putative immunoglobulin heavy constant gamma 1 (G1m marker)	IPi00645363	52 kDa	220	433	118	225	
56	Sushi domain-containing protein 2	IPi00021302	167 kDa	341	307	241	339	
57	Inter-alpha (globulin) inhibitor H2	IPi00645038	125 kDa	261	275	142	267	
58	Complement component C7	IPi00296608	94 kDa	256	214	275	243	
59	Isoform 2 of TSC22 domain family protein 1	IPi00019355	89 kDa	263	260	209	233	
60	Thrombospondin-1	IPi00296099	129 kDa	42	400	51	406	
61	Alpha-2-antiplasmin	IPi00879231	55 kDa	262	214	227	214	
62	Isoform 2 of Ig mu chain C region	IPi00896380	59 kDa	256	245	131	277	
63	Pigment epithelium-derived factor	IPi00006114	46 kDa	201	194	241	185	
64	Apolipoprotein E	IPi00021842	36 kDa	163	177	220	227	
65	Plasma kallikrein	IPi00654888	71 kDa	188	201	173	180	
66	IGK@ protein	IPi00784865	555 kDa	231	215	311	104	
67	Isoform 4 of Clusterin	IPi00976752	49 kDa	147	164	206	224	
68	Insulin-like growth factor-binding protein complex acid labile subunit isoform 1 precursor	IPi00925635	70 kDa	233	224	172	160	
69	252 kDa protein	IPi00022937	252 kDa	153	139	195	195	
70	Coagulation factor XII	IPi00019581	68 kDa	159	142	188	162	
71	Angiotensin II receptor	IPi00021438	113 kDa	151	322	110	227	

Author Manuscript

Author Manuscript

Author Manuscript

Author Manuscript

#	Identified Proteins (503)	IPI N.	MW	Female-day 1	Female day 5	Male day 1	Male day 5	
72	Lumican	IP00020986	38 kDa	201	169	205	180	
73	Isoform HMW of Kininogen-1	IP00032328	72 kDa	159	134	156	164	
74	Complement C1q subcomponent subunit B	IP00477992	27 kDa	151	166	171	101	
75	Isoform 1 of Inter-alpha-trypsin inhibitor heavy chain H3	IP00028413	100 kDa	145	124	126	105	
76	Talin-1	IP00298994	270 kDa	69	212	69	235	
77	Vitamin K-dependent protein S	IP00294004	75 kDa	139	90	120	96	
78	42 kDa protein	IP00942787	139 kDa	188	236	0	77	
79	Carboxypeptidase N subunit 2	IP00479116	61 kDa	159	139	131	134	
80	Serum amyloid P-component	IP00022391	25 kDa	99	95	166	127	
81	Kallistatin	IP00328600	76 kDa	129	124	159	120	
82	Leucine-rich alpha-2-glycoprotein	IP00022417	38 kDa	100	91	122	121	
83	Isoform 1 of Ficolin-3	IP00293925	33 kDa	133	121	145	110	
84	Complement component C8 gamma chain	IP00011261	22 kDa	158	122	157	118	
85	Putative Ig kappa chain V-II region RPM1 6410	IP00550731	26 kDa	0	0	139	331	
86	Complement component C9	IP00022395	63 kDa	130	85	138	109	
87	Isoform 1 of Filamin-A	IP00333541	343 kDa	65	239	27	165	
88	Thyroxine-binding globulin	IP00292946	46 kDa	140	121	100	69	
89	Isoform 2 of Inter-alpha-trypsin inhibitor heavy chain H4	IP00218192	101 kDa	119	134	112	101	
90	Isoform 1 of C4b-binding protein beta chain	IP00025862	115 kDa	102	87	116	97	
91	Isoform 2 of N-acetylmuramoyl-L-alanine amidase	IP00394992	68 kDa	118	102	103	102	
92	Putative immunoglobulin heavy constant gamma 2 (G2m marker)	IP00426051	51 kDa	137	215	0	0	
93	Complement component C8 beta chain	IP00294395	118 kDa	138	81	91	59	
94	Complement component C8 alpha chain	IP00011252	65 kDa	113	73	72	51	
95	Lambda-chain	IP00827875	25 kDa	86	82	117	131	
96	Isoform 3 of Attractin	IP00939169	134 kDa	54	63	93	97	
97	Isoform 5 of F-box only protein 11	IP00386876	171 kDa	135	64	115	12	
98	Carboxypeptidase N catalytic chain	IP00010295	52 kDa	105	100	81	76	
99	Corticosteroid-binding globulin	IP00027482	45 kDa	95	108	84	77	
100	Isoform 1 of Extracellular matrix protein 1	IP00003351	61 kDa	111	108	87	56	
101	CD5 antigen-like	IP00025204	108 kDa	77	88	47	52	
102	haaptoglobin isoform 2 preproprotein	IP00478493	38 kDa	0	0	129	179	
103	Coagulation factor X	IP00019576	55 kDa	65	51	88	61	
104	Putative immunoglobulin heavy constant gamma 1 (G1m marker)	IP00816314	51 kDa	0	3	111	155	
105	Serum paraoxonase/arylesterase 1	IP00218732	40 kDa	48	61	72	79	
106	Complement C2 (Fragment)	IP00303963	83 kDa	80	77	61	58	
107	Isoform 1 of Myosin-9	IP00019502	249 kDa	6	135	2	107	
108	Complement C1q subcomponent subunit C	IP00022394	26 kDa	57	61	85	68	
109	von Willebrand factor	IP00023014	309 kDa	11	48	39	162	
110	Tetranectin	IP00009028	23 kDa	55	38	79	61	
111	Hepatocyte growth factor activator	IP00029192	71 kDa	97	78	55	48	
112	Glutathione peroxidase 3	IP00026199	26 kDa	53	38	72	54	
113	Complement component 5 variant (Fragment)	IP00816741	123 kDa	96	111	7	27	
114	Isoform 2 of Apolipoprotein L1	IP00186903	46 kDa	37	48	50	58	
115	Mannose-binding protein C	IP00004373	26 kDa	30	18	82	69	
116	Hemoglobin subunit beta	IP00654755	16 kDa	27	26	103	120	
117	Complement C1q subcomponent subunit A	IP00022392	26 kDa	61	72	77	51	
118	Hyaluronan-binding protein 2	IP00746623	63 kDa	56	57	37	42	
119	Isoform Long of Complement factor H-related protein 2	IP00006154	31 kDa	38	35	52	60	
120	hepatocyte growth factor-like protein precursor	IP00925540	82 kDa	44	36	62	64	
121	Alpha-1-acid glycoprotein 2	IP00020091	24 kDa	57	53	66	73	
122	Galectin-3-binding protein	IP00023673	65 kDa	81	47	54	62	
123	Coagulation factor IX	IP00296176	52 kDa	42	24	66	34	
124	Coagulation factor XIII B chain	IP00007240	76 kDa	56	57	51	53	
125	Tyrosine-protein kinase receptor	IP00642703	328 kDa	5	3	14	171	
126	rab3 GTPase-activating protein catalytic subunit isoform 1	IP00927682	229 kDa	68	65	61	52	
127	Selenoprotein P	IP00029061	43 kDa	47	33	66	49	
128	Putative Putative uncharacterized protein DKFZp686I15212	IP00418153	57 kDa	35	58	47	44	
129	Isoform 1 of Alpha-actinin-1	IP00013508	103 kDa	12	101	18	75	
130	Isoform 1 of Carboxypeptidase B2	IP00329775	48 kDa	29	32	40	20	
131	Isoform C of Proteoglycan 4	IP00655976	141 kDa	16	50	38	30	
132	Oxysterol-binding protein	IP00911080	763 kDa	32	42	35	55	
133	Isoform 1 of Pregnancy zone protein	IP00025426	164 kDa	87	98	0	2	
134	Isoform 1 of Haptoglobin-related protein	IP00477597	39 kDa	29	39	44	59	
135	Plasma serine protease inhibitor	IP00007221	46 kDa	28	45	49	51	
136	Platelet basic protein	IP00022445	14 kDa	26	82	28	78	
137	Complement C4 gamma chain (C04A (Rodgers blood group))	IP00843913	193 kDa	0	174	8	8	
138	Adiponectin	IP00020019	26 kDa	49	32	44	35	
139	Isoform 2 of Fibrinogen alpha chain'	IP00029717	70 kDa	35	136	0	0	
140	IGL@ protein	IP00829640	25 kDa	15	32	54	49	
141	L-lactate dehydrogenase B chain	IP00219217	37 kDa	24	46	32	38	
142	Beta-Ala-His dipeptidase	IP00064667	57 kDa	72	44	42	19	
143	Complement factor D preproprotein	IP00165972	28 kDa	34	21	58	53	
144	Hemoglobin subunit alpha	IP00410714	15 kDa	12	14	53	71	

Author Manuscript

Author Manuscript

Author Manuscript

Author Manuscript

145	Apolipoprotein M	IP00030739	21 kDa	13	16	28	36	
146	Isoform 1 of Vinculin	IP00291175	117 kDa	12	58	12	52	
147	Coagulation factor XIII A chain	IP00297550	83 kDa	27	35	34	54	
148	Carbonic anhydrase 1	IP00215983	29 kDa	32	22	61	49	
149	Fructose-bisphosphate aldolase A	IP00465439	39 kDa	15	29	23	33	
150	Complement factor H-related protein 1	IP00011264	96 kDa	17	16	42	50	
151	Nucleosome assembly protein 1-like 4 (Fragment)	IP01010987	218 kDa	10	25	56	47	
152	Rheumatoid factor C6 light chain (Fragment)	IP00829956	13 kDa	31	26	31	28	
153	Isoform 1 of C-reactive protein	IP00022389	25 kDa	38	27	23	20	
154	calcium binding protein 39-like	IP00844534	54 kDa	0	76	23	64	
155	Putative immunoglobulin heavy constant alpha 1	IP00426060	136 kDa	19	65	21	22	
156	cDNA FLJ78387	IP00876888	52 kDa	6	67	0	53	
157	Inter-alpha-trypsin inhibitor heavy chain H3	IP01015883	380 kDa	28	21	20	25	
158	29 kDa protein	IP01014269	536 kDa	5	4	19	36	
159	Gamma-glutamyl hydrolase	IP00023728	36 kDa	41	38	28	16	
160	Isoform 1 of Tropomyosin alpha-4 chain	IP00010779	29 kDa	7	43	25	39	
161	Isoform 1 of Mannan-binding lectin serine protease 1	IP00299307	79 kDa	44	37	35	34	
162	Lambda light chain of human immunoglobulin surface antigen-related protein (Fragment)	IP00927263	25 kDa	33	47	39	28	
163	Isoform 1 of Sulfhydryl oxidase 1	IP00003590	83 kDa	26	30	38	29	
164	Isoform 1 of L-lactate dehydrogenase A chain	IP00217966	37 kDa	21	34	18	42	
165	Isoform 2 of Ficolin-3	IP00419744	32 kDa	31	31	25	30	
166	Isoform 1 of Coagulation factor XI	IP00008556	70 kDa	21	25	30	31	
167	Isoform 1 of Phosphatidylinositol-glycan-specific phospholipase D	IP00299503	92 kDa	13	17	41	60	
168	Isoform F of Proteoglycan 4	IP00656092	146 kDa	37	8	18	11	
169	14-3-3 protein zeta/delta	IP00021263	28 kDa	14	29	15	45	
170	Isoform 1 of Sex hormone-binding globulin	IP00023019	44 kDa	51	34	31	16	
171	IgGfc-binding protein*	IP00242956	572 kDa	37	22	29	13	
172	Isoform 3 of Muscular LMNA-interacting protein	IP00922212	319 kDa	29	13	22	11	
173	Insulin-like growth factor-binding protein 3	IP00018305	32 kDa	39	17	18	8	
174	Properdin	IP00021364	51 kDa	24	29	21	25	
175	Sodium/nucleoside cotransporter 2	IP00014561	126 kDa	11	66	8	47	
176	SAA2-SAA2 protein	IP00975939	23 kDa	18	24	35	32	
177	histone deacetylase 11	IP00879927	180 kDa	15	19	35	39	
178	cysteine-rich secretory protein 3 isoform 1 precursor	IP00942117	29 kDa	16	11	19	19	
179	Carbonic anhydrase 2	IP00218414	29 kDa	23	33	33	32	
180	Platelet glycoprotein Ib alpha polypeptide (Fragment)	IP00748955	70 kDa	25	44	16	34	
181	Apolipoprotein D	IP00006662	161 kDa	10	12	24	37	
182	Immunoglobulin J chain	IP00178926	18 kDa	26	24	19	24	
183	Profilin-1	IP00216691	15 kDa	14	29	10	36	
184	Fleckstrin	IP00306311	40 kDa	13	31	12	23	
185	Serglycin	IP00019972	18 kDa	0	22	0	24	
186	Apolipoprotein A-II*	IP00021854	11 kDa	19	28	22	21	
187	Isoform 2 of Serine/threonine-protein kinase LMTK1	IP00784827	109 kDa	10	48	11	14	
188	Isoform 4 of Adenylate kinase domain-containing protein 1	IP00930224	269 kDa	27	11	31	35	
189	Tumor necrosis factor receptor superfamily member 1A	IP01010586	156 kDa	45	0	30	0	
190	Peptidyl-prolyl cis-trans isomerase A	IP00419585	18 kDa	11	28	13	19	
191	10 kDa protein	IP01026484	84 kDa	24	7	14	8	
192	2-oxoglutarate and iron-dependent oxygenase domain-containing protein 2	IP01010230	111 kDa	15	21	18	17	
193	Lymphatic vessel endothelial hyaluronin acid receptor 1	IP00290856	110 kDa	17	21	19	20	
194	Isoform 1 of Complement factor B (Fragment)	IP00921523	86 kDa	15	11	42	18	
195	Ig kappa chain V-HV region Len	IP00387120	13 kDa	21	20	0	23	
196	Prolow-density lipoprotein receptor-related protein 1	IP00020557	505 kDa	28	21	18	16	
197	serine/threonine-protein kinase MARK2 isoform c	IP00902451	810 kDa	13	0	4	16	
198	Lysozyme C	IP00019038	17 kDa	6	12	16	22	
199	Complement C1r subcomponent-like protein	IP00009793	53 kDa	29	17	13	12	
200	ficolin (collagen/fibrinogen domain containing lectin) 2 (hucolin)	IP00871650	35 kDa	13	15	17	23	
201	Aminopeptidase N	IP00221224	110 kDa	11	19	26	19	
202	Isoform 2 of Tropomyosin alpha-3 chain	IP00218319	29 kDa	0	32	10	14	
203	Apolipoprotein C-IV	IP00022731	15 kDa	13	9	16	11	
204	Putative Putative uncharacterized protein	IP00807428	25 kDa	37	0	2	31	
205	Sphingomyelin phosphodiesterase 2	IP00017670	97 kDa	9	39	14	28	
206	Isoform 1 of Vascular cell adhesion protein 1	IP00018136	81 kDa	19	14	19	12	
207	Cation-independent mannose-6-phosphate receptor	IP00228919	274 kDa	14	6	22	24	
208	Isoform 2 of Inter-alpha-trypsin inhibitor heavy chain H3	IP00876950	299 kDa	30	21	0	3	
209	Dopamine beta-hydroxylase	IP00171678	69 kDa	28	20	19	11	
210	Cofilin-1	IP00012011	19 kDa	5	15	10	23	
211	Putative immunoglobulin heavy constant gamma 4 (G4m marker)	IP00930442	139 kDa	17	19	6	12	
212	Platelet factor 4	IP00022446	11 kDa	7	28	8	29	
213	Phosphoglycerate kinase	IP01011912	41 kDa	9	30	9	14	
214	24 kDa protein	IP00647915	90 kDa	7	21	14	26	
215	Apolipoprotein(a)	IP00029168	501 kDa	12	12	5	15	
216	Isoform 4 of Mannan-binding lectin serine protease 1	IP00924973	69 kDa	17	0	17	13	
217	Myosin-reactive immunoglobulin kappa chain variable region (Fragment)	IP00384401	12 kDa	4	5	4	8	

#	Identified Proteins (503)	IPI N.	MW	Female day 1	Female day 5	Male day 1	Male day 5	
218	Glutathione S-transferase omega-1	IPI00019755	28 kDa	12	20	12	19	
219	Monocyte differentiation antigen CD14	IPI00029260	40 kDa	17	17	25	21	
220	Immunoglobulin heavy chain variable region (Fragment)	IPI00783287	13 kDa	9	0	8	8	
221	Ig kappa chain V-I region AG	IPI00387022	12 kDa	22	20	12	21	
222	Ig kappa chain V-IV region JI	IPI00386132	15 kDa	14	17	18	7	
223	Isoform 1 of Tricosephosphate isomerase	IPI00797270	27 kDa	0	22	16	26	
224	Cystatin-C	IPI00032293	16 kDa	13	13	18	21	
225	Isoform 1 of Vitamin K-dependent protein Z	IPI00027843	45 kDa	13	6	11	4	
226	Apolipoprotein C-I	IPI00021855	9 kDa	14	15	15	17	
227	Fatulin-B	IPI00743766	42 kDa	14	19	13	13	
228	Single-chain Fv (Fragment)	IPI00748998	26 kDa	0	0	3	3	
229	Cold agglutinin FS-1 L-chain (Fragment)	IPI00827273	12 kDa	15	6	7	10	
230	Vasorin	IPI00395488	72 kDa	14	11	13	10	
231	L-selectin precursor	IPI00218795	44 kDa	16	11	9	7	
232	Sarcoma antigen NY-SAR-29 (Fragment)	IPI00384443	88 kDa	17	33	4	12	
233	Isoform 3 of Neural cell adhesion molecule 1	IPI00220737	84 kDa	8	4	16	13	
234	Isoform 1 of Tenascin	IPI00031008	268 kDa	13	14	18	19	
235	CD1c molecule	IPI00514282	105 kDa	5	0	7	0	
236	Glyceraldehyde-3-phosphate dehydrogenase	IPI00219018	36 kDa	0	14	5	19	
237	Isoform 1 of Peptidase inhibitor 16	IPI00301143	49 kDa	14	22	15	9	
238	Protein interacting with PRKCA 1	IPI00893321	139 kDa	6	3	4	5	
239	UGa8H (Fragment)	IPI00828099	13 kDa	17	32	6	0	
240	Isoform 1 of Cartilage acidic protein 1	IPI00451624	71 kDa	13	11	15	13	
241	Insulin-like growth factor-binding protein 2 precursor	IPI00297284	35 kDa	5	10	16	8	
242	Chloride intracellular channel protein 1	IPI00010896	77 kDa	10	21	9	21	
243	Isoform 2 of cAMP-dependent protein kinase catalytic subunit alpha	IPI00217960	103 kDa	0	17	4	21	
244	Extracellular superoxide dismutase [Cu-Zn]	IPI00027827	26 kDa	13	11	15	8	
245	Similar to Ig kappa chain V-III region VG precursor	IPI00977405	12 kDa	12	5	10	13	
246	Paralemmin-2	IPI00643947	81 kDa	0	0	4	47	
247	Pantetheinase	IPI00030871	57 kDa	12	10	13	11	
248	Integrator complex subunit 7 isoform 4	IPI00909591	263 kDa	4	6	13	11	
249	Leukocyte elastase inhibitor	IPI00027444	138 kDa	5	15	0	5	
250	Dipeptidyl peptidase 4	IPI00018953	88 kDa	11	5	4	3	
251	Myosin-reactive immunoglobulin light chain variable region (Fragment)	IPI01025882	12 kDa	12	0	11	22	
252	Platelet glycoprotein V	IPI00027410	61 kDa	2	25	0	31	
253	Isoform 4 of Rho guanine nucleotide exchange factor 7	IPI00449909	158 kDa	12	9	6	7	
254	Apolipoprotein C-III	IPI00021857	11 kDa	14	10	12	8	
255	Secreted phosphoprotein 24	IPI00011832	24 kDa	10	5	11	11	
256	Ferroxidoxin_2	IPI00027350	22 kDa	5	3	19	17	
257	Peptidylglycine alpha-amidating monooxygenase	IPI00749176	273 kDa	0	16	24	0	
258	Isoform XB of Tenascin-X	IPI00025276	464 kDa	4	2	20	17	
259	Coactosin-like protein	IPI00017204	16 kDa	4	17	0	12	
260	Isoform 1 of Multiple epidermal growth factor-like domains protein 8	IPI00027310	303 kDa	21	18	4	6	
261	Isoform 1 of 14-3-3 protein epsilon	IPI00000816	29 kDa	6	14	12	10	
262	Angiogenin	IPI00008554	17 kDa	8	9	11	12	
263	Isoform D of Fibulin-1	IPI00296534	77 kDa	15	0	7	17	
264	Isoform 3 of Ectonucleotide pyrophosphatase/phosphodiesterase 2	IPI00878576	102 kDa	16	9	12	8	
265	Fructose-bisphosphate aldolase B	IPI00218407	39 kDa	14	11	8	0	
266	Gelsolin	IPI01009415	165 kDa	5	8	8	0	
267	Isoform 1 of Cell surface glycoprotein MUC18	IPI00016334	72 kDa	10	7	12	9	
268	Similar to VH4 heavy chain variable region precursor	IPI00977297	15 kDa	0	8	0	3	
269	Isoform 2 of Mannan-binding lectin serine protease 2	IPI00306378	21 kDa	6	7	0	3	
270	Isoform 2 of Gelsolin	IPI00646773	81 kDa	0	0	18	0	
271	Ceramide synthase 3	IPI00796378	70 kDa	13	15	0	13	
272	Isoform 1 of Multimerin-1	IPI00012269	138 kDa	4	4	3	13	
273	Ig mu heavy chain disease protein	IPI00385264	43 kDa	33	0	0	0	
274	tudor domain containing 1	IPI00908751	534 kDa	0	3	5	3	
275	Rho GDP-dissociation inhibitor 2	IPI00003817	23 kDa	4	8	3	5	
276	23 kDa protein	IPI01025316	23 kDa	4	0	5	0	
277	13 kDa protein	IPI00829803	13 kDa	6	7	5	10	
278	Isoform APP770 of Amyloid beta A4 protein (Fragment)	IPI00006608	87 kDa	0	11	0	18	
279	Isoform 2 of Neural cell adhesion molecule L1-like protein	IPI00299059	137 kDa	13	9	7	2	
280	Peptidyl prolyl cis-trans isomerase B	IPI00646304	24 kDa	3	20	2	16	
281	Apolipoprotein C-II	IPI00021856	11 kDa	10	8	10	4	
282	Metalloproteinase inhibitor 1	IPI00032292	23 kDa	0	11	0	3	
283	Isoform 1 Soluble scavenger receptor cysteine-rich domain-containing SSCSD	IPI00979213	166 kDa	8	12	16	8	
284	Xaa-Pro dipeptidase	IPI00257882	55 kDa	9	8	15	9	
285	Isoform alpha-enolase of Alpha-enolase	IPI00465248	47 kDa	0	15	5	14	
286	Isoform 1 of Spermatogenesis-associated protein 24	IPI00940491	86 kDa	35	0	0	0	
287	Eas suppressor protein 1	IPI00017256	32 kDa	0	14	0	9	
288	GPI ethanolamine phosphate transferase 2 (Fragment)	IPI00966518	148 kDa	0	6	0	25	
289	Bone marrow proteoglycan	IPI00010341	25 kDa	5	0	8	10	
290	minichromosome maintenance complex component 5	IPI00878128	130 kDa	4	0	4	0	

Author Manuscript

Author Manuscript

Author Manuscript

Author Manuscript

#	Identified Proteins (503)	IPIN	MW	Female day 1	Female day 5	Male day 1	Male day 5	
291	Fibrinogen gamma chain*	IP100877703	63 kDa	0	26	4	0	
292	Ig lambda chain V region 4A	IP10022890	12 kDa	3	4	0	5	
293	Tubulin alpha-1C chain	IP100218343	50 kDa	2	15	0	19	
294	Phosphatidylethanolamine-binding protein 4	IP100163563	26 kDa	4	0	4	2	
295	Similar to Ig kappa chain V-IV region JI precursor	IP100549330	14 kDa	8	8	8	8	
296	Uncharacterized protein	IP101022408	11 kDa	0	11	7	9	
297	CD44 antigen (CDw44) (Epicam) (Extracellular matrix receptor III) (ECMR-III) (GP90)	IP100984539	79 kDa	2	0	6	5	
298	Myosin-reactive immunoglobulin light chain variable region	IP101026045	12 kDa	0	6	0	0	
299	Ig kappa chain V-III region S6	IP100387113	46 kDa	7	6	13	7	
300	Collagen alpha-1(I) chain	IP100297646	139 kDa	4	0	14	0	
301	Interleukin-33 isoform 2 precursor	IP100908682	170 kDa	0	0	30	0	
302	Insulin-like growth factor-binding protein 6	IP100029235	25 kDa	11	9	11	9	
303	Isoform 1 of Integrin alpha-1Ib	IP100295976	113 kDa	0	26	0	10	
304	Transaldolase	IP100744692	38 kDa	3	14	6	5	
305	Anti-streptococcal/anti-myosin immunoglobulin lambda light chain variable region (Fragment)	IP100956602	12 kDa	5	3	6	0	
306	Ig kappa chain V-I region DEE	IP100387025	12 kDa	0	3	0	5	
307	Isoform C of Fibulin-1	IP100296537	74 kDa	3	13	7	0	
308	Similar to Kappa light chain variable region	IP100924820	13 kDa	0	5	0	0	
309	Ig lambda chain V-III region SH	IP100382436	11 kDa	8	6	0	5	
310	Phosphatidylcholine-sterol acyltransferase	IP100022331	50 kDa	13	6	3	2	
311	Moesin	IP100219365	68 kDa	2	12	0	0	
312	cDNA FLJ52091	IP100910161	412 kDa	7	4	3	0	
313	chromosome 11 open reading frame 51	IP100022312	103 kDa	0	0	4	4	
314	Endothelial protein C receptor precursor	IP100099276	31 kDa	0	6	9	3	
315	Collagen alpha-1(XVII) chain	IP101014165	178 kDa	0	5	6	4	
316	Lipopolysaccharide-binding protein	IP100032311	53 kDa	4	5	4	8	
317	Isoform 2 of Fermitin family homolog 3	IP100216699	105 kDa	0	16	0	9	
318	Isoform 5 of Protein FRA10AC1	IP100429179	111 kDa	0	3	0	0	
319	Glutathione S-transferase P	IP100219757	23 kDa	0	9	3	9	
320	Tropomyosin 1 alpha variant 6	IP100384369	29 kDa	0	13	0	11	
321	Ankyrin 3 isoform 1 variant (Fragment)	IP101015955	364 kDa	0	10	0	0	
322	Anti-(ED-B) scFv (Fragment)	IP100916434	25 kDa	4	3	0	4	
323	Transferrin receptor protein 1	IP100022462	85 kDa	3	3	10	11	
324	Isoform 1 of Scavenger receptor cysteine-rich type 1 protein M130	IP100104074	125 kDa	5	5	8	5	
325	Protein AMN1 homolog (Fragment)	IP101012771	261 kDa	0	11	3	0	
326	apolipoprotein L1 isoform c precursor	IP100914948	324 kDa	0	0	7	3	
327	Protein S100-A8	IP100007047	11 kDa	4	0	0	3	
328	Ribosomal protein L18	IP100908950	377 kDa	9	0	12	0	
329	cDNA FLJ57278	IP100910763	878 kDa	0	0	3	0	
330	Fumarylacetoacetase	IP100031708	46 kDa	12	5	4	3	
331	Cryocryoglobulin CC1 kappa light chain variable region (Fragment)	IP100890703	12 kDa	8	0	0	0	
332	ADP-ribosyl cyclase 2	IP100026240	36 kDa	6	0	8	4	
333	Isoform 2 of Multimerin-1	IP100745154	58 kDa	0	16	0	9	
334	Isoform 4 of Latent-transforming growth factor beta-binding protein 1	IP100973177	187 kDa	0	3	0	17	
335	Isoform 1 of Mannan-binding lectin serine protease 2	IP100294713	76 kDa	0	0	7	0	
336	Isoform 1 of A disintegrin and metalloproteinase with thrombospondin motifs 13	IP100449028	154 kDa	4	8	0	0	
337	Plasminogen activator inhibitor 1	IP100007118	45 kDa	0	8	0	5	
338	Isoform 1 of NIF3-like protein 1	IP100694624	42 kDa	3	0	6	0	
339	Retinoic acid receptor responder protein 2	IP100019176	19 kDa	5	8	5	4	
340	polycystic kidney and hepatic disease 1 (autosomal recessive)-like 1	IP100940315	466 kDa	0	3	0	9	
341	Adenylyl cyclase-associated protein	IP101009563	308 kDa	0	7	0	3	
342	Dermcidin	IP100027547	11 kDa	0	0	7	3	
343	Peroxisomal protein 6	IP100220301	25 kDa	0	5	0	4	
344	BAI1-associated protein 3 isoform 4	IP100910379	261 kDa	0	0	3	0	
345	similar to mCG22736; similar to testicular serine protease 2	IP100918000	671 kDa	0	0	0	14	
346	Transforming growth factor beta-1	IP100000075	44 kDa	0	6	0	5	
347	Isoform 1 of Neutrophil gelatinase-associated lipocalin	IP100299547	23 kDa	3	3	6	6	
348	Cathelicidin antimicrobial peptide precursor	IP100292532	20 kDa	0	0	9	10	
349	Isoform 2 of Nidogen-1	IP100384542	122 kDa	0	3	0	9	
350	Isoform 2 of UPF0577 protein KIAA1324	IP100643029	179 kDa	3	3	0	2	
351	Vacuolar protein sorting 72 homolog	IP100844510	128 kDa	0	3	0	2	
352	Procollagen C-endopeptidase enhancer 1	IP100299738	48 kDa	3	0	8	8	
353	cDNA FLJ53559	IP100908874	296 kDa	0	0	15	0	
354	Inter-alpha (Globulin) inhibitor H4 (Plasma Kallikrein-sensitive glycoprotein) variant (Fragment)	IP101018048	77 kDa	0	0	0	3	
355	Macrophage colony-stimulating factor 1 receptor	IP100011218	108 kDa	4	5	0	0	
356	Isoform 3 of Histone-lysine N-methyltransferase SETDB1	IP100879832	228 kDa	0	7	0	0	
357	Flavin reductase	IP100783862	22 kDa	0	0	7	6	
358	Protein DJ-1	IP100298547	20 kDa	0	0	0	7	
359	Isoform 6 of ADP-dependent glucokinase	IP100903303	205 kDa	0	3	3	3	
360	Creatine kinase M-type	IP100027487	43 kDa	0	0	2	6	
361	Alpha-amylase 1	IP100300786	58 kDa	0	0	0	10	
362	Isoform 2 of WD repeat-containing protein 1	IP100903292	248 kDa	0	9	0	0	
363	Membrane primary amine oxidase	IP100004457	85 kDa	4	5	4	3	

#	Identified Proteins (503)	IP1 N	MW	Fema	Reday 4	Day 5	Male day 1	Male day 5	
364	Ig lambda-2 chain C region	IP100642632	50 kDa	0	0	0	4	4	
365	V3-3 protein	IP100553092	37 kDa	0	0	0	3	0	
366	Annexin A5	IP100329801	36 kDa	0	13	0	0	0	
367	fibronectin 1	IP100873210	286 kDa	0	0	0	0	14	
368	Isoform 2 of Alpha-1B-glycoprotein	IP100644018	41 kDa	3	4	0	0	4	
369	Actin-related protein 2/3 complex subunit 1B	IP100005160	41 kDa	0	9	0	0	5	
370	Ig lambda chain V-II region BUR	IP100003947	12 kDa	3	0	0	0	0	
371	Isoform 1 of Adenylyl cyclase-associated protein 1	IP100008274	52 kDa	0	9	0	0	3	
372	Gamma-aminobutyric acid receptor subunit beta-1	IP100299122	126 kDa	0	13	0	0	0	
373	78 kDa glucose-regulated protein	IP100003362	72 kDa	2	8	0	0	0	
374	Tubulin beta-1 chain	IP100006510	50 kDa	0	2	0	0	11	
375	Cryocystoglobulin CC2 lambda light chain variable region (Fragment)	IP100890733	11 kDa	0	0	0	5	3	
376	Isoform 1 of Noelin	IP100017841	55 kDa	0	0	0	2	3	
377	Periodic tryptophan protein 2 homolog (Fragment)	IP100797937	49 kDa	0	0	0	0	4	
378	Zinc finger protein 487	IP100916109	197 kDa	0	8	0	0	7	
379	12 kDa protein	IP100892569	12 kDa	4	5	3	0	0	
380	Actin-related protein 2/3 complex subunit 2	IP100005161	34 kDa	0	3	0	0	6	
381	Peptidyl-prolyl cis-trans isomerase (Fragment)	IP101013799	97 kDa	0	0	0	16	0	
382	LIM and senescent cell antigen-like-containing domain protein 1	IP100788612	37 kDa	0	6	0	0	2	
383	complement factor H	IP100218999	51 kDa	0	0	0	4	0	
384	Isoform 1 of Trem-like transcript 1 protein	IP100410333	33 kDa	0	0	0	0	6	
385	Tropomyosin isoform	IP100018853	28 kDa	0	4	0	0	0	
386	V5-6 protein	IP100478997	13 kDa	0	4	0	0	4	
387	Isoform 2 of Proteasome subunit alpha type-3	IP100171199	79 kDa	4	4	3	0	0	
388	V2-7 protein	IP100747252	13 kDa	5	4	0	0	0	
389	CD9 antigen	IP100215997	25 kDa	0	3	0	0	0	
390	Isoform LAMP-2A of Lysosome-associated membrane glycoprotein 2	IP100009030	45 kDa	5	6	3	0	0	
391	eukaryotic peptide chain release factor GTP-binding subunit ERF3A isoform 2	IP100905083	442 kDa	6	0	0	0	0	
392	31 kDa protein	IP101010884	116 kDa	0	11	0	0	0	
393	Ras-related protein Rap-1b	IP100015148	21 kDa	0	0	0	0	11	
394	Cerebellin-4	IP100018396	22 kDa	0	0	0	3	0	
395	Isoform 1 of Contactin-1	IP1002029751	113 kDa	0	3	4	0	0	
396	exostosins (multiple)-like 2	IP100640272	36 kDa	4	3	4	0	0	
397	Actin-related protein 2	IP100005159	45 kDa	0	5	0	0	0	
398	Cathepsin D	IP100011229	45 kDa	0	0	0	8	5	
399	Platelet glycoprotein Ib alpha	IP100943099	73 kDa	0	0	0	0	6	
400	Ubiquitin (Fragment)	IP101014596	94 kDa	0	4	0	0	4	
401	Isoform 2 of Peptidase inhibitor 16	IP100845506	30 kDa	7	0	0	3	0	
402	Collectin-10	IP100007917	31 kDa	4	0	0	0	0	
403	Ribonuclease 4	IP100029699	17 kDa	2	2	7	0	0	
404	VK3 protein (Fragment)	IP100827830	208 kDa	0	0	0	3	0	
405	Alpha-N-acetylglucosaminidase	IP100008787	82 kDa	3	0	0	2	4	
406	complement factor H-related protein 4 isoform 1 precursor	IP100985459	65 kDa	0	0	0	4	4	
407	Collagen alpha-2(I) chain	IP100304962	129 kDa	0	0	0	8	0	
408	Beta-2-microglobulin	IP100004656	211 kDa	0	0	0	12	0	
409	Immunoglobulin heavy chain variable region	IP100854743	13 kDa	0	3	0	0	0	
410	acyl-CoA synthetase short-chain family member 2	IP100945625	79 kDa	3	5	0	0	2	
411	Ig lambda chain V-II region TRO	IP100382420	12 kDa	0	3	0	0	0	
412	Integrin beta	IP101015923	84 kDa	0	9	0	0	4	
413	Protein S100-A9	IP100027462	13 kDa	3	0	0	2	3	
414	Endoplasmic	IP100027230	92 kDa	0	4	2	2	2	
415	Isoform 2 of Mast/stem cell growth factor receptor	IP100848233	109 kDa	0	0	0	4	0	
416	Dehydrogenase/reductase SDR family member 4-like 2 (NADPH)-dependent retinol dehydrogenase/red	IP101012232	88 kDa	4	4	0	0	0	
417	Di-N-acetylchitinase	IP100007778	44 kDa	0	0	0	3	0	
418	V2-17 protein	IP100550162	12 kDa	0	0	0	0	3	
419	Isoform 1 of Nucleoside diphosphate kinase B	IP100026260	17 kDa	0	0	0	0	2	
420	Isoform 2 of Plexin-B1	IP100006644	214 kDa	2	0	0	0	0	
421	Amyloid lambda 6 light chain variable region SAR (Fragment)	IP101022820	12 kDa	0	0	0	0	3	
422	complement factor H-related protein 3 isoform 2 precursor	IP100908535	64 kDa	0	0	0	2	0	
423	Isoform 2 of Receptor-type tyrosine-protein phosphatase gamma	IP100796281	159 kDa	0	2	4	0	0	
424	Ig kappa chain V-III region IARC/BL41	IP100386131	14 kDa	3	0	0	0	4	
425	Ig lambda chain V-II region LOI	IP100385985	12 kDa	4	2	0	0	0	
426	Isocitrate dehydrogenase [NADP] cytoplasmic	IP100027222	126 kDa	0	3	0	0	0	
427	Angiotensin-related protein 3	IP100004957	54 kDa	3	6	0	0	0	
428	PDZ and LIM domain protein 1	IP100010414	36 kDa	0	0	0	4	3	
429	Calreticulin	IP100020599	48 kDa	0	5	0	0	0	
430	Bone marrow proteoglycan precursor	IP100847535	57 kDa	0	6	0	0	0	
431	I4-3-3 protein gamma	IP100220642	28 kDa	0	6	0	0	2	
432	plexin domain containing 2	IP100640599	58 kDa	0	0	0	2	2	
433	Cathepsin Z	IP100002745	34 kDa	0	0	0	4	3	
434	Inhibin beta C chain	IP100023314	38 kDa	0	0	0	0	3	
435	Plastin-2	IP100010471	70 kDa	4	0	0	0	0	
436	Interferon regulatory factor 2	IP100293657	110 kDa	0	4	0	0	0	

Author Manuscript

Author Manuscript

Author Manuscript

Author Manuscript

Author Manuscript

Author Manuscript

Author Manuscript

Author Manuscript

#	Identified Proteins (503)	IPI_N	MW	Female day 1	Female day 5	Male day 1	Male day 5	
437	Immunoglobulin heavy chain	IPI00735451	13 kDa	4	0	0	0	
438	Isoform 10 of Fibronectin	IPI00497923	240 kDa	0	3	0	3	
439	neuropilin 1	IPI00639917	79 kDa	0	0	3	0	
440	Ig lambda chain V-I region NEW	IPI00382421	11 kDa	0	3	0	0	
441	Ribonuclease pancreatic	IPI00014048	18 kDa	0	0	4	0	
442	Isoform 2 of Insulin-like growth factor II	IPI00940065	20 kDa	0	0	4	3	
443	388 kDa protein	IPI01009607	388 kDa	4	2	0	0	
444	Zymogen granule protein 16 homolog B	IPI00060800	23 kDa	0	0	0	7	
445	dystrophin Dp140c isoform	IPI00376375	203 kDa	0	6	0	0	
446	Ig kappa chain C region	IPI00909649	162 kDa	0	5	0	0	
447	Isoform beta of Poliovirus receptor	IPI00219425	40 kDa	3	0	2	0	
448	Ig kappa chain V-III region GOL	IPI00385252	12 kDa	0	4	0	0	
449	Rho GDP-dissociation inhibitor 1	IPI00003815	23 kDa	0	3	0	0	
450	Phosphoglycerate mutase 1	IPI00549725	29 kDa	0	3	0	5	
451	Galectin-related protein	IPI00023549	19 kDa	0	4	0	0	
452	Apolipoprotein F	IPI01012338	33 kDa	0	0	4	3	
453	Alpha-mannosidase 2	IPI00003802	131 kDa	0	6	0	0	
454	14-3-3 protein eta	IPI00216319	28 kDa	0	0	0	6	
455	Superoxide dismutase [Cu-Zn]	IPI00218733	16 kDa	0	3	0	0	
456	calumenin isoform c precurosor	IPI00789155	38 kDa	0	5	0	0	
457	Isoform short of 14-3-3 protein beta/alpha	IPI00759832	28 kDa	0	9	0	0	
458	Isoform Beta-3A of Integrin beta-3	IPI00503283	87 kDa	0	8	0	0	
459	Thymus specific serine peptidase	IPI00385292	123 kDa	0	5	0	0	
460	Proteasome subunit beta type-2	IPI00028006	23 kDa	0	2	0	0	
461	Myosin-reactive immunoglobulin heavy chain variable region (Fragment)	IPI00384407	14 kDa	0	2	0	0	
462	Endonuclease domain-containing 1 protein	IPI00001952	55 kDa	0	3	0	0	
463	Isoform 1 of Putative chromosome 9 open reading frame 92	IPI00647376	42 kDa	0	0	0	3	
464	Similar to V1-5 protein	IPI00553215	13 kDa	0	3	0	0	
465	Isoform M1 of Pyruvate kinase isozymes M1/M2	IPI00220644	58 kDa	0	0	0	3	
466	Multimerin-2	IPI00015525	104 kDa	0	3	0	3	
467	14-3-3 protein theta	IPI00018146	28 kDa	0	0	0	2	
468	Isoform 1 of Bridging integrator 2	IPI00505092	62 kDa	0	4	0	2	
469	Cadherin-1	IPI00025861	97 kDa	3	4	0	0	
470	Polymeric immunoglobulin receptor	IPI00004573	83 kDa	0	2	0	0	
471	Isoform 1 of DDB1- and CUL4-associated factor 8	IPI00290071	205 kDa	0	4	0	0	
472	Isoform 3 of Protocadherin-8	IPI00910395	354 kDa	0	4	0	0	
473	Coronin-1C_13 protein	IPI00867509	59 kDa	0	5	0	0	
474	Ig alpha-1 chain C region	IPI00978930	54 kDa	0	0	0	5	
475	Ceruloplasmin (Fragment)	IPI00879084	57 kDa	0	3	2	0	
476	Protein shisa-7	IPI00917604	76 kDa	0	0	0	4	
477	Synaptotagmin-7 (Fragment)	IPI01012979	86 kDa	0	2	0	0	
478	Isoform 1 of Complement C1q tumor necrosis factor-related protein 3	IPI00008860	27 kDa	4	0	0	0	
479	Isoform 1 of Attractin	IPI00027235	159 kDa	0	0	4	0	
480	SH3 domain-binding glutamic acid-rich-like protein 2	IPI00412272	12 kDa	0	0	0	5	
481	Thyrotropin-releasing hormone-degrading ectoenzyme	IPI00007798	117 kDa	3	0	0	0	
482	F-box only protein 2	IPI01018924	79 kDa	0	0	3	0	
483	Isoform 1 of Nucleoside diphosphate kinase A	IPI00012048	17 kDa	0	4	0	0	
484	14-3-3 protein zeta/delta (Fragment)	IPI01011530	62 kDa	0	3	0	0	
485	P-selectin	IPI00295339	91 kDa	0	2	0	0	
486	GRB10 interacting GYF protein 2	IPI00915868	47 kDa	0	0	3	0	
487	Cathepsin S	IPI00299150	37 kDa	3	0	0	0	
488	Glutamyl aminopeptidase	IPI00014375	109 kDa	2	0	2	0	
489	74 kDa protein	IPI01011336	306 kDa	0	0	0	3	
490	Vasodilator-stimulated phosphoprotein	IPI00301058	40 kDa	0	5	0	0	
491	Isoform Non-muscle of Myosin light polypeptide 6	IPI00335168	17 kDa	0	4	0	0	
492	Isoform 1 of Insulin-like growth factor II	IPI00001611	115 kDa	4	0	0	0	
493	HRV Fab N27-VL (Fragment)	IPI00827560	12 kDa	0	5	0	0	
494	MHC class II antigen (Fragment)	IPI00645451	136 kDa	0	0	0	2	
495	cDNA FLJ51171	IPI00910239	422 kDa	3	0	0	0	
496	Actin-related protein 2/3 complex subunit 4	IPI00554811	20 kDa	0	0	0	4	
497	Cryocrystalglobulin CCl1 heavy chain variable region (Fragment)	IPI00890754	13 kDa	0	2	0	0	
498	Isoform 2 of Tropomodulin-2	IPI00908786	251 kDa	0	0	0	2	
499	N(4)-(beta-N-acetylglucosaminy)-L-asparaginase	IPI00026259	37 kDa	0	0	3	0	
500	V4-2 protein	IPI00830107	13 kDa	0	0	0	2	
501	galactose-3-O-sulfotransferase 4	IPI00925529	120 kDa	0	3	0	0	
502	Isoform 11 of Dysferlin	IPI00910624	321 kDa	0	0	0	3	
503	Isoform 1 of CD166 antigen	IPI00015102	65 kDa	2	0	0	0	

* proteins are partially depleted through Top14 plasma protein depletion column